

UNIVERSIDADE DE SÃO PAULO
ESCOLA POLITÉCNICA
DEPARTAMENTO DE ENGENHARIA DE MINAS E DE PETRÓLEO

LEONARDO FONSECA REGINATO

**Application of machine learning techniques for modeling of relative permeability in
engineered water injection in carbonate reservoirs**

São Paulo

2022

LEONARDO FONSECA REGINATO

**Application of machine learning techniques for modeling of relative permeability in
engineered water injection in carbonate reservoirs**

Original Version

Dissertation presented to the Graduate Program in Mineral Engineering at Polytechnic School, University of São Paulo to obtain the degree of Master of Science.

Concentration Area: Mineral Engineering

Advisor: Prof. Marcio Augusto Sampaio Pinto, PhD

São Paulo

2022

Nome: REGINATO, Leonardo Fonseca

Título: Application of Machine Learning Techniques for Modeling of Relative Permeability in Engineered Water Injection in Carbonate Reservoirs

Dissertação apresentada ao Departamento de Engenharia de Minas e de Petróleo da Universidade de São Paulo para obtenção do título de Mestre em Ciências.

Aprovado em:

Banca Examinadora

Prof. Dr.

Instituição:

Julgamento:

ACKNOWLEDGEMENTS

I would like to thank my family and friends who have always been by my side supporting me throughout my path.

I thank my girlfriend, Ingrid V. Bunholi, who has always been by my side during my academic journey.

Thanks to my advisor Prof. Marcio Augusto Sampaio for accepting to conduct my research work.

I also want to thank the University of São Paulo and all the professors of my course for the high quality of teaching offered, in particular the group Laboratory of Petroleum Reservoir Simulation and Management (LASG) and Integrated Technology for Rock and Fluid Analysis (InTRA) for providing the required infrastructure to perform this research.

“Intelligence is the ability to adapt to change.”

(Stephen Hawking)

ABSTRACT

REGINATO, Leonardo Fonseca. **Application of machine learning techniques for modeling of relative permeability in engineered water injection in carbonate reservoirs**. 2022. 82 p. Dissertation (Master's in Science) - Escola Politécnica, Universidade de São Paulo, São Paulo, 2022.

Numerical modeling of advanced production methods is always a challenge to be developed and applied in reservoir simulation. Some approaches, such as the use of laboratory experiments, arise to make this modeling feasible. However, this limits the speed of the solution to obtaining laboratory data and impairs its reproducibility. With the increasing use of Machine Learning (ML) tools to solve complex non-linear problems, we conducted these studies to train these ML tools and couple them to commercial simulation software. The training was based on parameters relevant to Engineered Water Injection (EWI). This advanced injection method seeks to use salinity control in the injection water to promote interactions between its ions and the rock minerals, to facilitate its flow into the porous medium. Thus, we structured a dataset containing salinity, mineralogy, and relative permeability data for the data-driven ML tool to learn the behavior of this data. Thus, this approach achieves accurate predictions, which were used as input data during injection modeling and simulation, validating its results by comparing with production simulation by conventional geochemical modeling. Finally, we performed optimizations with waterflooding injection and EWI, coupling the optimization with the advanced method of the ML pipeline. Thus, we test the efficiency of the ML approach with recursive simulations and compare the efficiency between the injection methods. For this, we apply these optimizations to the UNISIM-II benchmark, a reservoir model with characteristics based on Brazilian Pre-Salt fields. The objective function was Net Present Value maximization, which for the tests performed, EWI presented higher profit, even with a cost margin up to 300% higher than the cost of waterflooding.

Keywords: Engineered Water Injection; Numerical Simulation; Carbonates; Machine Learning; Optimization.

RESUMO

REGINATO, Leonardo Fonseca. **Aplicação de técnicas de aprendizado de máquina para modelagem da permeabilidade relativa na injeção de água calibrada em reservatórios carbonáticos**. 2022. 82 p. Dissertação (Mestrado em Engenharia Mineral) – Escola Politécnica, Universidade de São Paulo, São Paulo, 2022.

A modelagem numérica de métodos avançados de produção sempre é um desafio para ser desenvolvida e aplicada na simulação de reservatórios. Algumas abordagens como o uso de resultados laboratoriais surgem para tentar viabilizar essas modelagens. Porém, isso limita a velocidade da solução a obtenção do dado laboratorial e prejudica sua reprodutibilidade. Com o crescente uso de ferramentas de Aprendizado de Máquina (do inglês *Machine Learning* – *ML*) para solução de problemas complexos e não lineares, nos conduzimos esses estudos para treinar essas ferramentas e acoplá-las a um software comercial de simulação. O treinamento baseava-se nos parâmetros relevantes para a injeção de água calibrada (do inglês *Engineered Water Injection* – *EWI*). Esse método de injeção avançada busca utilizar o controle de salinidade na água de injeção para promover interações entre seus íons e os minerais da rocha, para facilitar seu escoamento no meio poroso. Assim, estruturamos um conjunto de dados que contém dados de salinidade, mineralogia e permeabilidade relativa para a ferramenta ML guiada pelos dados aprender o comportamento desses dados. Assim, essa abordagem foi capaz de fazer previsões precisas, que foram utilizadas como dados de entrada durante a modelagem e simulação da injeção, validando seus resultados comparando com a simulação da produção pela modelagem geoquímica convencional. Por fim, realizamos otimizações com injeção de água comum e *EWI*, acoplando na otimização com o método avançado o pipeline de *ML*. Assim, testamos a eficiência da abordagem *ML* com simulações recursivas e comparamos a eficiência entre os métodos de injeção. Para isso, aplicamos essas otimizações no benchmark UNISIM-II, um modelo de reservatório com características baseadas em campos do Pré-Sal brasileiro. A função objetivo foi a maximização do Valor Presente Líquido, que para os testes realizados a *EWI* apresentou maior lucro, mesmo com uma margem de custo de até 300% superior ao custo da injeção de água comum.

Palavras-chave: Injeção de Água Projetada; Simulação Numérica; Carbonatos; Aprendizado de Máquinas; Otimização.

LIST OF FIGURES

Figure 1: Artificial neuron structure.	19
Figure 2: a - Initial K centroids randomly; b - After the training process the clusters are defined.....	21
Figure 3: Workflow of general methodology.....	28
Figure 4: Relative Permeability Module procedure.	30
Figure 5: Workflow of Relative Permeability module coupled to FGA algorithm.	31
Figure 6: Illustrative structure of the database for ANN training separated into input and output data.	32
Figure 7: Architecture of feedforward network, (a) input layer; (b) hidden layer, and (c) output layer.....	33
Figure 8: Cut model from USINIM-II-D, showing the porosity parameter.	39
Figure 9: Comparison with the prediction performance network varying the number of hidden neurons and learning algorithms	41
Figure 10: Normalized Mean Squared Error (nMSE) of Oil/Water Production between Conventional Simulation and Simulation with Net15_BR coupled.	42
Figure 11: Simulation Results, comparing the traditional EW Simulation and Simulation with Net15_BR relative permeability results.....	43
Figure 12: Simulation time comparison between the ANN coupling solution and conventional geochemical modeling.	44
Figure 13: Ionic concentration of water injection obtained by the optimization process.	46
Figure 14: Relative permeability of Engineered Water Optimized versus Normal relative permeability.....	47
Figure 15: KrModule Schema.....	53
Figure 16: ML Hybrid method overview.....	55
Figure 17: PSO with HML coupling workflow	57
Figure 18: Reduced Unisim-II model.....	59
Figure 19: PCA plot segmented by clusters.....	61
Figure 20: Centroids Clusters as Relative Permeability.....	62
Figure 21: Net 00 R2 score vs hidden layers number using grid search CV.....	64
Figure 22: Cross-plot predicted vs actual values.	65

Figure 23 (a, b, and c): Comparison of Kr-Curve predicted by each network (green) and the actual curves (black).....	65
Figure 24: Percent volume of fluids.	67
Figure 25: Optimized injection salinity.	68
Figure 26: Relative Permeability after optimization vs original.	69
Figure 27: Average water saturation during production.....	69
Figure 28: Study Case plane 17 of 30, cell saturation at 23/09/2046.....	71

SUMMARY

CHAPTER 1 – INTRODUCTION.....	16
1.1 Method of LSWI/EWI.....	16
1.2 Numerical Modeling EWI.....	17
1.3 Machine Learning.....	18
1.4 Motivation.....	21
1.5 Objectives.....	21
1.6 Dissertation Overview.....	22
CHAPTER 2 – OPTIMIZATION OF IONIC CONCENTRATIONS IN ENGINEERED WATER INJECTION IN CARBONATE RESERVOIR THROUGH ANN AND FGA	24
2.1 INTRODUCTION.....	24
2.2 METHODOLOGY.....	27
2.2.1 Conventional EWI Modeling and Simulation.....	28
2.2.2 Database for Neural Network Training.....	29
2.3 Neural Net Fitting Features.....	33
2.4 FGA and NNF Coupling.....	34
2.5 Case Studies.....	35
2.5.1 Engineered Water Conventional Simulation Features.....	35
2.5.2 Optimization Settings.....	37
2.5.3 UNISIM-II Benchmark.....	38
2.6 Results and Discussion.....	40
2.6.1 Validation of Network Predictions.....	40
2.7 Optimization Results.....	44
2.8 Conclusions.....	48
2.9 ACKNOWLEDGMENTS.....	49

CHAPTER 3 - HYBRID MACHINE LEARNING TO MODELING THE RELATIVE PERMEABILITY CHANGES IN CARBONATE RESERVOIRS UNDER ENGINEERED WATER INJECTION.....	50
3.1 INTRODUCTION	50
3.2 METHODOLOGY	52
3.2.1 Data Collection	52
3.2.2 KrModule Procedure.....	53
3.2.3 Hybrid Machine Learning Method.....	54
3.2.4 EWI and Water Optimization	56
3.3 CASE STUDY	58
3.3.1 UNISIM-II Benchmark.....	58
3.3.2 KrModule PSO Parameters	60
3.4 RESULTS AND DISCUSSION	60
3.4.1 K-Means Clusterization Results	60
3.4.2 Neural Network Results.....	63
3.4.3 Optimizations	66
3.5 CONCLUSIONS	71
3.6 ACKNOWLEDGMENTS	71
CHAPTER 4 – CONCLUSIONS	73
BIBLIOGRAPHY	75

CHAPTER 1 – INTRODUCTION

Reservoir production has three main stages: (i) primary production, which makes use of the reservoir's natural energy; (ii) secondary, which uses external water or gas injection for pressure maintenance and (iii) tertiary, which develop injection fluids that promote physicochemical iterations to facilitate oil displacement.

Primary and secondary methods recover on average 60% of the oil volume in place. Usually, after many years of production via these methods, some tertiary injection (a.k.a. Enhanced Oil Recovery - EOR) is applied. However, this may reduce the recovery potential of the EOR method, which could be better performance when implemented earlier (BAI, 2008; BABADAGLI, 2020).

In carbonates, the use of advanced injection methods is attractive due to the high complexity of their petrophysical conditions, which are close to a third of the volume of oil recovered with primary and secondary methods (AUSTAD et al., 2015; CHANDRASEKHAR; MOHANTY, 2018; KAZEMI et al., 2014).

Water injection is the most widely implemented recovery method in the world. In offshore conditions, this method has an advantage in raw material availability, reliability, and profitability. Usually, injected seawater treatments are made to promote compatibility with the rock, avoiding formation damage. To improve the technique efficiency, some authors have applied experiments to investigate the hypothesis of changing the composition of the brine to increase the injection efficiency (DANG et al., 2013).

1.1 Method of LSWI/EWI

Bernard published some of the first research in 1976 investigating the effects promoted in sandstone samples by freshwater injection. He hypothesized that hydratable clays reacted with the injected water to alter the properties of the rock samples. Morrow et al. (1998) analyzed the interactions of brine salinity with crude oil, mineralogy, and wettability settings. More recently, a series of analyses involving the topic has emerged to determine the potentials of each mechanism involving the injection (JERAULD et al., 2008; MORROW et al., 1998; WEBB et al., 2004; ZHANG et al., 2006).

In the last two decades, some mechanisms found through the Low Salinity Water Injection (LSWI) include fines migration, wettability alteration, multi-component ionic exchange (MIE), pH modification, and electrical double layer effect. Also, these effects can occur in combination during the injection (DANG et al., 2013).

In some cases, high salinities concentrations perform better, especially in carbonates. Thus, an update of the method is proposed, called Engineered Water Injection (EWI) (AL-SHALABI et al., 2015; CHANDRASEKHAR; MOHANTY, 2018; WEBB et al., 2005; ZHANG et al., 2007).

The EWI assumptions are the same as the LSWI, but for the new method, the range of ions is higher, finding an optimal solution for each application. The works that have investigated injection define three ions (SO_4^{2-} , Ca^{2+} , and Mg^{2+}) as the principal agents for changes to a more hydrophilic rock condition. Sulfate is the wettability modifying agent in carbonates, and the other two divalent cations (calcium and magnesium), promote strong interactions with the oil components (ADEGBITE et al., 2018; REGINATO et al., 2021; STRAND et al., 2006; WEBB et al., 2005; YOUSEF et al., 2012).

Wettability alteration is one of the fundamental mechanisms of LSWI/EWI application. Through the shape of the relative permeability curves, it is possible in qualitative analysis to classify this type of change, which produces an impact on oil and water permeability during injection (ALZAYER; SOHRABI, 2013; BRODIE; JERAULD, 2014; FJELDE et al., 2012; REGINATO et al., 2019; WEBB et al., 2008).

1.2 Numerical Modeling EWI

Modeling the behavior of fluids considering these effects of ionic interactions is complex due to their nonlinear nature. Moreover, it is a multi-scale problem, which increases the difficulty of coupling the solution. Therefore, are develop few studies focusing on solving such complexities for the simulation environment (ESENE et al., 2018).

Jerauld et al. (2008) presented one of the first modeling approaches for LSWI. In that work, they show a simple correlation between the relative permeability and capillary pressure as a function of salinity. In 2012, Omekeh et al. presented a model of ion exchange and mineral solubility with LSWI. This approach had a standard oil condition

(Black-Oil), and the ions present in the composition were sulfate, calcium, magnesium, and sodium. The permeability change occurs in the function of ion exchange between the fluid and the rock surface.

Dang et al. (2013) aggregate the aqueous and mineral interactions for their solution. They develop an ion-exchange model considering both situations, updating to multi-component compositions as well. Computer Modelling Group (CMG) commercial software uses that approach to modeling the LSWI behaviors. However, the solution needs experimental data to complete the geochemical modeling, requiring specific laboratory tests to collect this information.

The numerical solution of LSWI/EWI is currently limited to complex approaches and laboratory experiments. Therefore, using new tools to incorporate the effects of salinity on wettability can bring new modeling perspectives. Hence, this work uses Artificial Intelligence (AI) tools capable of learning the relationship between the parameters involved in the injection with a simple approach. This training process, when well employed, allows accurate and agile predictions, reducing the numerical solution time compared to geochemical modeling.

1.3 Machine Learning

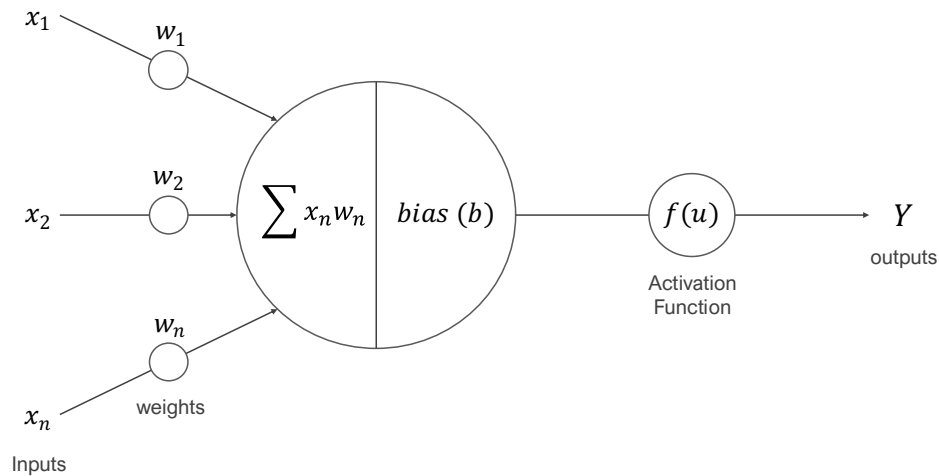
Artificial Intelligence (AI) technologies have gained considerable attention over the years due to their simple implementation, easy adaptation to different problems, and robust generalization capabilities (EVANS, 2019; SIRCAR et al., 2021). AI is defined by the ability of machines to replicate attributes of the human brain. Thus, these tools are programmed not to solve specific problems but to learn with data, enabling them to solve more complex problems (MALEKIAN; CHITSAZ, 2021).

Machine learning (ML) is an AI application in which it uses data-driven mathematical tools, widely used in data forecasting (YASEEN et al., 2015). Artificial Neural Networks (ANNs) are one of the types of ML algorithms, which are inspired by brain biology (MOHAGHEGH; AMERI, 1995). Their training defines a pattern among information, generating an empirical relationship between the data during the training process. Thus, ANNs are a powerful tool for prediction in data-dependent problems where

internal physics or the relationship between the data is complex for a conventional solution (GOVINDARAJU; RAO, 2013; MALEKIAN; CHITSAZ, 2021; NGUYEN et al., 2020).

Artificial Neural Networks have nodes, artificial neurons, interconnect by coefficients (weights), composing the neural structure. The neuron operation initially receives the signals (input), multiplies them by their respective weights, and sums them up. Then the result goes through the activation function producing the output (Figure 1). The structure of an ANN has three main layers: input layer, hidden layer, and output layer. Therefore, the information (data) propagates from the input to output direction, making its training iteratively adjust the weights of each neuron, minimizing the error between the output and the actual value (AGATONOVIC-KUSTRIN; BERESFORD, 2000).

Figure 1: Artificial neuron structure.



Source: Perform by the Author.

So, this mathematical relationship of the ANN model is expressed by the equation below:

$$Y = b + \sum_{n=1}^m W_n X_n \quad (1)$$

Equation 1: Artificial neuron equation.

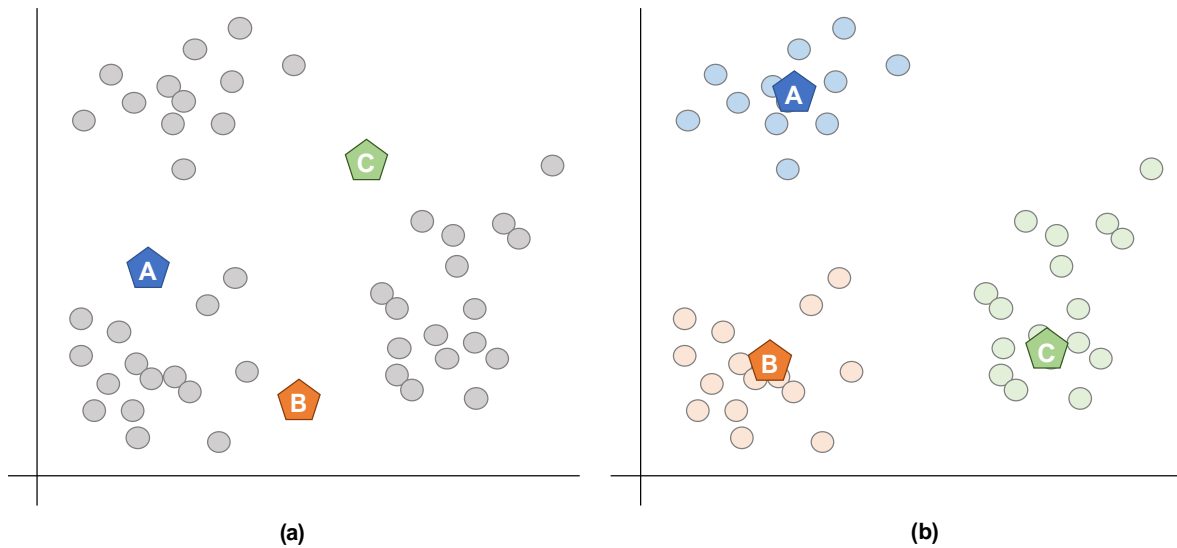
Where X , input; Y , output; b , bias; m , number of inputs and W , weight. The activation function is responsible for the neuron activation or not. Thus, its purpose is to add nonlinearity to the output. The most common functions include logistic sigmoid and hyperbolic tangent (AGATONOVIC-KUSTRIN; BERESFORD, 2000; ARAGHINEJAD, 2014; MALEKIAN; CHITSAZ, 2021).

ML algorithms are divided into two learning methods, supervised and unsupervised. Supervised are those that need the output (or target) for accurate outcome prediction. Unsupervised learning aims to find patterns only based on unlabeled data. These unsupervised algorithms are powerful for finding hidden patterns in high numbers of features configuration without human intervention (LEE et al., 2005; MALEKIAN; CHITSAZ, 2021).

Clustering is one of the applications for unsupervised ML models. This technique is one of the most common applications of data analysis. Its training process aims to generate a new set of categories through the similarity of the data, and this new data subset promotes more robust data analysis, allowing for multi-variable pattern observation (LIKAS et al., 2003; MADHULATHA, 2012).

K-means clustering is a type of unsupervised learning with the goal is to cluster the unlabeled data based on the similarity between features. Initially, the number of K clusters is defined, and the algorithm randomly inserts K centroids into the space of variables. Then, the algorithm goes through the data measuring the Euclidean distance between them and the centroids (similarity). Then, iteratively, these centroids are repositioned (Figure 2) until be in the average position of each region which the density of objects is high (MADHULATHA, 2012; MORISSETTE; CHARTIER, 2013).

Figure 2: a - Initial K centroids randomly; b - After the training process the clusters are defined.



Source: Perform by Author.

1.4 Motivation

Current modeling techniques for engineered water injection require complex geochemical solutions and specific laboratory data. Therefore, we use a Machine Learning (ML) procedure to learn the relationship between salinity, mineralogy, and relative permeability. Thus, we have a simple solution to coupling in simulation software, and easy to implement, requiring less petrophysical experimental data. In addition, this workflow development becomes powerful for studies with the injection method, which sometimes has no previous analysis of fluids and rock behavior in specific conditions.

1.5 Objectives

This work aims to develop an EWI simulation pipeline with coupling machine learning tools to reproduce the wettability alteration by predicting relative permeability behavior. That produces an alternative approach for modeling the advanced injection

method behavior, which simplifies the numerical solution and reduces the amount of input data. Also, we apply an optimization process, validating the approach performance and comparing the results between common water injection and EWI by maximizing the Net Present Value (NPV).

1.6 Dissertation Overview

Four chapters divide this work, relating two complementary approaches for modeling the effects of EWI using ML prediction tools. In addition, is employed an optimization process comparing the production simulation results between common water injection and EWI.

Chapter 2 presents the first approach to developing a machine learning algorithm of the Artificial Neural Network type. Its learning used the injection concentrations (Ca, Mg and SO_4^{2-}) and the relative permeability curves, seeking to predict the behavior of the wettability alteration. Thus, we used a synthetic database for training, validating its production simulation with conventional geochemical modeling. Finally, we apply optimization of ordinary water injection and EWI to maximize the NPV of a case study. In this step, we validate the quality and agility of the predictions of the ANN coupled to optimization in the EWI case, then compare the performance between the two recovery methods. About the case study, for efficiency in the simulation time, we cut a portion of the proposed benchmark, the Unisim-II, with reduced dimensions of 6x6x30 cells, considering its economic scenario proportional to its cut size.

In the third chapter, we expanded the current methodology through hybrid machine learning (HML) solution. In this approach, we first use an unsupervised classifier module (K-Means) to segment between 3 types of relative permeability, then three neural networks of the same type are trained using the data from each cluster. Thus, we developed more expert ANNs in each cluster label to improve the prediction performance due to increased training parameters, which in this case was: formation salinity (SO_4 , Ca, Mg, Na, Cl), mineralogy (calcite and dolomite), injection salinity (SO_4 , Ca, Mg, Na, Cl), and relative permeability. In this step, we also test the simulation pipeline coupling the new HML in the optimization process. Thus, we note the advantages of adding the

classifier before the predictions and the three expert neural networks in each condition, using the same reduced case study.

In the final chapter, we show the conclusions from the previous two chapters, discussing the improvements of the methodology with ML applied in the first step compared to conventional geochemical modeling. Then, we see the advantages in expanding this methodology and increasing the complexity of the problem through HML.

CHAPTER 2 – OPTIMIZATION OF IONIC CONCENTRATIONS IN ENGINEERED WATER INJECTION IN CARBONATE RESERVOIR THROUGH ANN AND FGA

Abstract

Engineered Water Injection (EWI) has been increasingly tested and applied to enhance fluid displacement in reservoirs. The modification of ionic concentration provides interactions with the pore wall, which facilitates the oil mobility. This mechanism in carbonates alters the natural rock wettability being quite an attractive recovery method. Currently, numerical simulation with this injection method remains limited to simplified models based on experimental data. Therefore, this study uses Artificial Neural Networks (ANN) learnability to incorporate the analytical correlation between the ionic combination and the relative permeability (K_r), which depicts the wettability alteration. The ionic composition in the injection system of a Brazilian Pre-Salt benchmark is optimized to maximize the Net Present Value (NPV) of the field. The optimization results indicate the EWI to be the most profitable method for the cases tested. EWI also increased oil recovery by about 8.7% with the same injected amount and reduced the accumulated water production around 52%, compared to the common water injection.

2.1 INTRODUCTION

Reservoir engineering seeks to manage the entire productive life of the field. This requires using computational tools to find the best strategy and to guarantee the highest NPV. Its simulation requires parameters, such as physical, chemical, petrophysical, extension, localization, and architecture. Thus, knowing these conditions and considering economic scenarios, it is possible to decide on a better oil recovery method.

These numerical models seek to be the best real reservoir representation, but often some information is disregarded to enable the simulation, which generates unreliable forecasting data to outline a successful strategy in the production of this field. According to Fabri et al. (2020), one solution is to calibrate the simulation with experimental work, but this can provide an increase in computational effort. Thus, it is ideal to use simulation

tools that preserve its real characteristics, especially when combined with advanced production methods (BREITENBACH, 1991; LIE, 2019; MUSTAFIZ; ISLAM, 2008).

Some oil recovery methods have gained attention, such as Low Salinity Water Injection (also called Smart Waterflood (Saudi Aramco), Designer Water (Shell), LoSal (British Petroleum), and Advanced Ion Management (ExxonMobil)). In general terms, Low Salinity Water Injection (LSWI) is an enhanced technique in which the ionic concentration control of injected water results in additional oil recovery of the field (DANG et al., 2015). After intensive laboratory research and field-scale tests with LSWI achieve positive responses, the method is currently accepted and applied by major oil companies worldwide (ZHANG et al., 2020).

This technique appears in one of the first surveys by Bernard (1967), who observed a different oil recovery in the tested samples, just varying the injected brine composition. The author hypothesizes that this effect happens in the interaction with freshwater and hydratable clay present in sandstone samples. In 1998, Morrow et al., quantified the influence of brine composition in the wettability properties, using the spontaneous imbibition core test, beginning the discussion on a multi-effect occurring during the water, oil, and rock interaction.

Other works confirm the LSWI as an appropriate application in carbonate reservoirs, in which the main effect reported was the reduction of the polar bond between carboxylic compounds and rock minerals, increasing the pore wall water adsorption (STRAND et al., 2006; ZHANG et al., 2007; YOUSEF et al., 2010; FATHI et al., 2011). Therefore, the control of potential ions (SO_4^{2-} , Mg^{2+} , and Ca^{2+}) results in a modification of natural wettability characteristics. Thus, the Wettability Alteration (WA) to more water-wet conditions is a crucial parameter to decrease the residual oil saturation (HIRASAKI *et al.*, 2004; SEETHEPALLI et al., 2004; WEBB et al., 2004; SAIKIA et al., 2018). Zaheri et al. (2020) perform coreflooding analysis with carbonates using LSWI. They observed a relation between higher calcium content in formation water and a more oil-wet condition. They also noted the calcium concentration reduction and the sulfate presence affected the ultimate oil recovery.

According to Adegbite et al.(2017), wettability alteration is the main reason for incremental oil recovery by LSWI in carbonate reservoirs. Also, they suggest a new

tendency to adapt the original ionic composition with a higher salinity range for each application. Through this concept, an update in the LSWI was generated, called Engineered Water Injection (EWI). Following the same hypothesis of the predecessor method, the differences are in raising the salinity limits, enabling to use higher ions concentrations.

Regarding the EWI method, a number of researches use an experimental approach to replicate the flow conditions in the reservoir and to determine the fundamental mechanism present in the analysis. Several works classify the effect of wettability alteration, fines migration, multi-component ionic exchange (MIE), pH modification, effect salt-in, contact angle measurement, electrical double layer and interfacial tension as the main effects (JERAULD et al., 2006; DANG et al., 2016; GHOSH et al., 2016; BIDHENDI et al., 2018; XIAO et al., 2018). According to different authors, it is possible to represent wettability alteration through changes in the relative permeability curves (JERAULD et al., 2008; FATHI et al., 2011; YOUSEF et al., 2011; REGINATO et al., 2019). Wettability alteration is extensively investigated to understand the influence in the oil and water behavior, being directly relevant to the macroscopic relative permeability (ZHANG et al., 2020).

The combination of these main mechanisms in EWI has a complex numerical background, making rare the development of analytical models capable of depicting this injection scheme. Therefore, it was common to use a simple relationship as a linear function among salinity, relative permeability, and capillary pressure (DANG et al., 2013). To enhance this modeling, researchers of the Computer Modeling Group (CMG), the University of Calgary and University of Texas at Austin developed a new complete approach that translated some present mechanisms of LS injection, using some experimental results as input data to perform the simulations (DANG et al., 2016). The authors sought to couple some equations from exclusively geochemical software to a compositional flow simulator. Even knowing the numerical limitations, the authors proposed to validate this coupling by comparing the results of experimental injections in a coreflooding system (FJELDE et al., 2012). This test obtained quite significant results in this coupling to the flow simulator. Another aspect of the existing models for LSW/EWI

simulation is a simplistic assumption whose change in wettability implies only in the modification of two-phase flow parameters (BOURBIAUX, 2020).

In most cases, the specific parameters required by simulation software to model the EWI are unknown, which makes this analytical tool useless without an initial experimental analysis. Thus, to provide an alternative to model this advanced injection with the absence of a laboratory data source, our study performs the training of a machine learning tool called Neural Net Fitting (NNF) that can reliably predict wettability changes considering a given salinity combination and relative permeability set in numerical simulation scale.

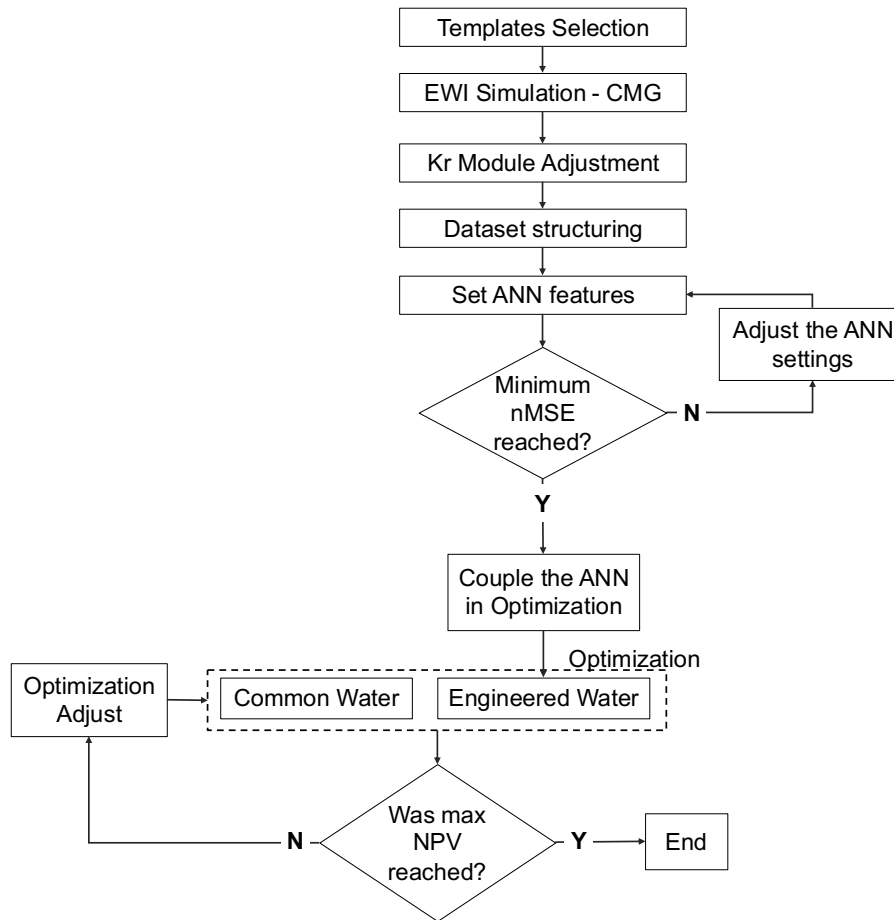
Moreover, we carry out an NPV maximization in a case study benchmark called UNISIM-II (CORREIA et al., 2015). The ionic concentration of water injected is optimized by the Fast-Genetic Algorithm (FGA), which provides the economic analysis of EWI and common water injection.

2.2 METHODOLOGY

As this work was performed only in a computational environment, it was necessary to use synthetic information to compose the database for future neural network training; therefore, some templates provided by CMG® were selected. We simulated these templates using EWI geochemical modeling with different salinity for each case through conventional software (compositional simulator). After that, a specific algorithm (Kr-Module) adjusted the initial relative permeability curves of a regular template until obtaining the same production simulation with geochemical modeling. The database generated was composed of the original Kr and corresponding salinity case as input and the newfound Kr curve as output, starting the network development. At the training stage, we tested different network patterns up to the maximum forecasting quality, based on statistical tools. The network provided a new Kr curve through the original curve and a given salinity. Then, we coupled the best neural network to the simulation, performing the validation by comparing the production outcome between the geochemical simulation (modeled in the CMG software) and the ANN.

Finally, ensuring the reliable application of the neural network, we coupled it to the optimization phase with the Fast Genetic Algorithm (FGA) to maximize the profits considering a range of costs, concluding the workflow (Figure 3).

Figure 3: Workflow of general methodology.



Source: Perform by Author.

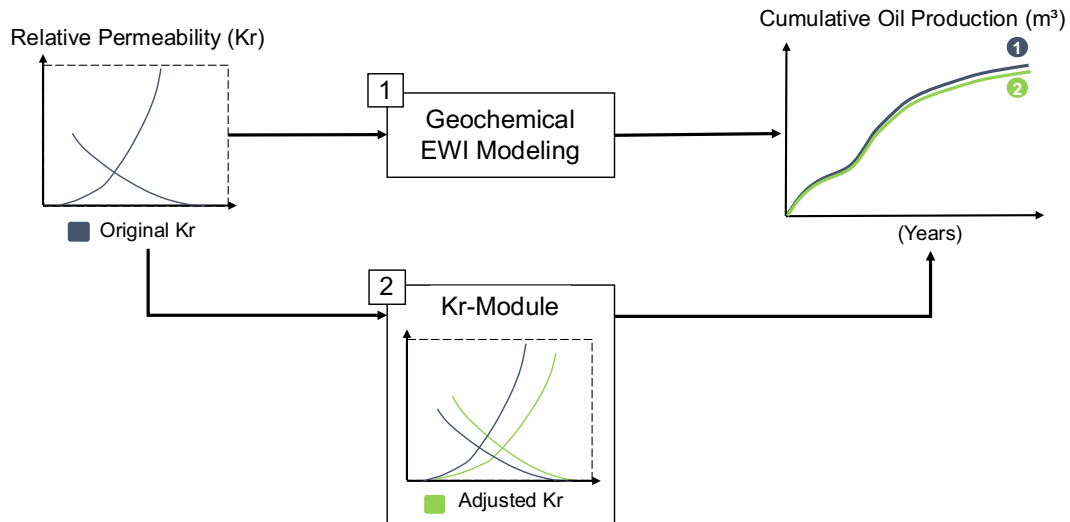
2.2.1 Conventional EWI Modeling and Simulation

In Both modeling ways (geochemical EWI and coupled by ANN) use the CMG software for simulation. The software requires informing the initial geochemical conditions of the EWI, such as the modeling method, the formation water salinity, the geochemical reactions considered and rock mineralogy. All the simulated cases keep the same input parameters, assigning the injection salinity as the only change agent in the production outcome.

2.2.2 Database for Neural Network Training

The database consists of 19 synthetic reservoir models selected from the CMG collection, from which the similarity with carbonate petrophysics and the possibility to apply the EWI modeling were the criteria to choose on these templates. Some of these are based on the SPE comparative solution project, which are generic benchmarks developed through experimental data and used to compare simulation performance or practice the functions of the software. Their particularities were also maintained, such as the wells position, flow rates, grid size, oil composition, and others, for a better network generalization, so that the results used in training were comprehensive in the reservoir configuration. Each template received the EWI modeling 15 times with random salinity, totalizing 285 cases. We defined the database structure with original Kr curves, their corresponding salinity, and the new Kr curve produced from conventional EWI. However, the commercial software becomes limited in the initial Kr curves and does not provide the state of the curve after the simulation. Thus, to generate this information, we developed the algorithm called Relative Permeability Module. This code aims to minimize the error between productions of the same template with and without EWI modeling, assigning adjustments to the Kr model curve without EWI to reduce this error (Figure 4). In practice, the Kr-Module adjusts the relative permeability of the model until the production result with the altered Kr curve be equal to the EWI. Thus, the new Kr correlates with the production change simulated by the EWI method and its salinity used.

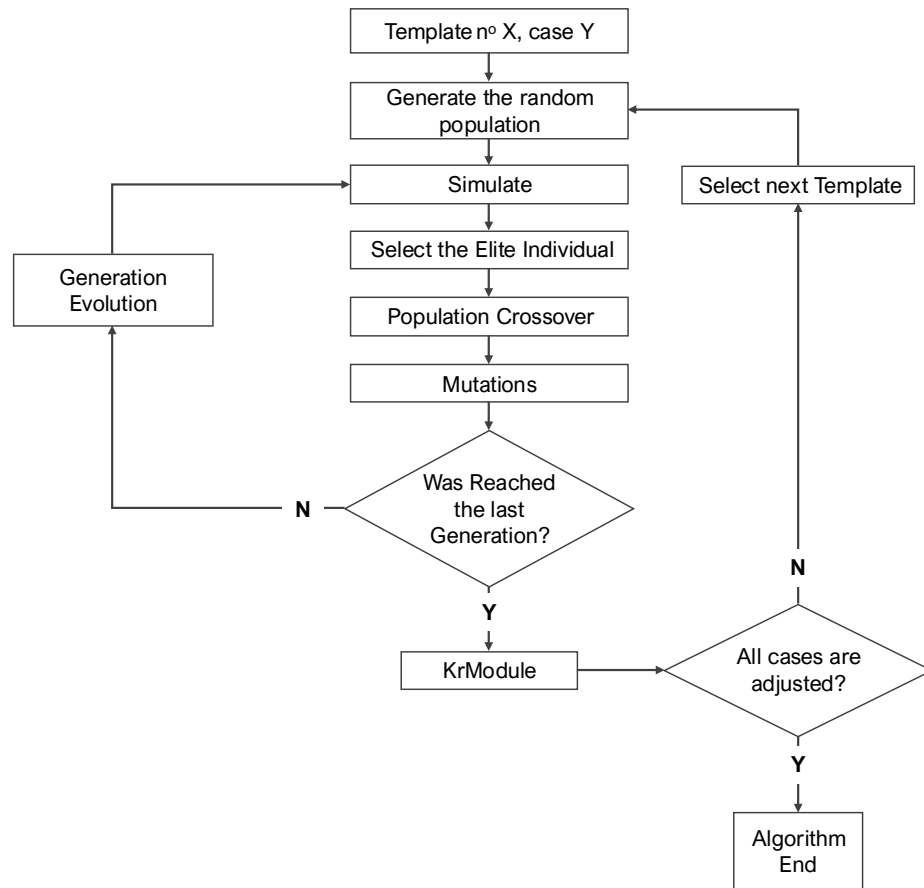
Figure 4: Relative Permeability Module procedure.



Source: Perform by Author.

This module was coupled with the Fast Genetic Algorithm (SAMPAIO et al., 2015) but adapted to minimize the error between the expected and simulated production outcomes, as shown in Figure 5. The algorithm inspiration is the evolution of a population through the generations (as in natural selection) using crossover and mutation until achieving the best solution (elite individual); in this case, it is the result with a minimum of the normalized Mean Squared Error (nMSE). Thus, the code requires the number of generations and quantities of individuals for generations to run. This code presents improvements in its solution speed, working with advanced modules and enhancing the simple crossover, parent selection, and evaluation function types.

Figure 5: Workflow of Relative Permeability module coupled to FGA algorithm.



Source: Perform by Author.

Recursively, the algorithm performed the adjustments to each specified model, saving its results in the database. We also converted the Kr curve into Corey equation parameters (Equations 2 and 3), establishing as input the original Kr-Corey parameters, their corresponding potential ion concentration and output the changed Kr-Corey parameters (Figure 6). This Kr curve transformation was necessary following the network-training criteria to reduce repeated data. The dataset parameters were selected to achieve the best of the neural network training. Therefore, the initial conditions (Swc and Kro at Swc) of multiple reservoir types were included to contribute to the improvement in the ANN performance.

Figure 6: Illustrative structure of the database for ANN training separated into input and output data.

	Input Parameters								Output Parameters				
	No	Nw	Sorw	Scw	...	SO ₄ ²⁻	Mg ²⁺	Ca ²⁺	No	Nw	Sorw	Scw	...
Tpl-1 EW1	3.4	2.3	0.7	0.2	...	9783	8744	2376	3.2	2.0	0.6	0.3	...
Tpl-1 EW2	2.5	4.3	0.5	0.1	...	3265	6431	3489	1.3	3.5	0.8	0.1	...
...
Tpl-1 EWn	3.1	3.7	0.9	0.17	...	4354	9822	3245	2.5	3.1	0.7	0.2	...

Source: Perform by Author.

Thus, the number of input parameters was equal to 12 with 8 for the Corey equation, 3 to salinity concentration, and 1 to salt interpolator. The output corresponded to 8 from the Corey equation. Brooks and Corey (1964) developed the equations below to allow calculating the permeability of a fluid at a given saturation that the medium is at the reference fluid.

$$k_{ro} = k_{rocw} \left(\frac{1 - S_w - S_{or}}{1 - S_{cw} - S_{or}} \right)^{n_o} \quad (2)$$

$$k_{rw} = k_{rwor} \left(\frac{S_w - S_{wcrit}}{1 - S_{wcrit} - S_{or}} \right)^{n_w} \quad (3)$$

where Equation 2 is for oil relative permeability and Equation 3 for water relative permeability of Corey formulation.

The parameters used in the network training are:

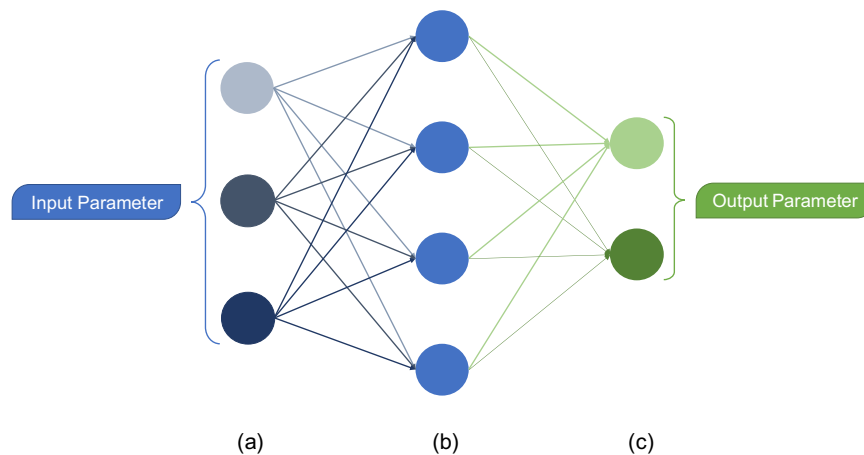
- k_{rocw} – Relative permeability of oil with connate water condition;
- k_{rwor} - Relative permeability of water in oil residual condition;
- S_w – Water saturation;
- S_{or} – Residual oil saturation;
- S_{cw} – Connate water saturation;
- S_{wcrit} – Critical water saturation;
- n_o – Corey exponent of oil;

- N_w – Corey exponent of water.

2.3 Neural Net Fitting Features

The best ANN following the MATLAB® applications for prediction purposes was the Neural Net Fitting (NNF) that can solve the data fitting problem using a simple architecture named feedforward. Mohaghegh (2000) defined the feedforward network as a set of neurons grouped in layers, where they usually consist of an input layer, hidden layer and output layer, as shown in Figure 7. The number of input neurons is equal to the number of parameters presented to the network; this also happens in the output layer, and the hidden layer can vary in neurons or layers. This interconnected system and composed of neurons works in three main steps: multiplication, sum and activation. The neuron multiplies each input data with its respective weight, sums these results, and uses a filter called the Activation Function (STRIK et al., 2005).

Figure 7: Architecture of feedforward network, (a) input layer; (b) hidden layer, and (c) output layer.



Source: Perform by Author.

This ANN uses a supervised learning method, which generally performs its training process combining the input data with the output (or labels), facilitating the creation of regression or classification, and indicating a quantitative relationship between them. Yet the limitation is that the training database needs to be complete, without missing data

(GHAHRAMANI, 2004; TALABIS et al., 2015; RAJASEKARAN; VIJAYALAKHMI PAI, 2017; SHOBHA; RANGASWAMY, 2018).

Another important aspect of configuring the network is its training algorithm, for which we opted for the Bayesian Regularization (BR). We performed some training tests with the other methods available, but both these results and theoretical concepts of the BR method converged to its use. This method is a mathematical process to adapt a nonlinear regression to statistical problems (well-posed). The robustness of the model minimizes the effect of overtraining or overfitting and has an automatic relevance determination (ARD). The ARD calculates the relevance for each input parameter, neglecting the irrelevant or highly correlated indexes (BURDEN; WINKLER, 2008). The Bayesian Regularized ANN (BRANNs) incorporates probabilistic interpretation into the regularization scheme. The regularization is a method to penalize the highest and the smallest weight in the neuron network and to ensure the best generalization (KAYRI, 2016). According to the MATLAB® guide, this BRANNs algorithm is slower in learning because at each learning epoch, the algorithm performs the relevance analysis, reducing the training speed but conserves the quality of the forecast, being ideal in training cases with a low number of samples, a high number of variables and non-linearity.

We also carried out another training test looking for the number of neurons in the hidden layer that would guarantee the maximum forecasting quality. We tested five different configurations (12, 15, 17, 20, and 25), and the results with 15 neurons in the hidden layer showed the best performance. All training followed a cross-validation process with the same configuration (70% of the data for training, 15% for validation and 15% for testing); 30 samples of the UNISIM-II case study (CORREIA et al., 2015) were generated to serve as a second validation of each network test, using the error between the expected and predicted result as a quality analysis. Thus, the best network was called “Net15_BR”.

2.4 FGA and NNF Coupling

To assess the economic attractiveness of EWI, we carried out a process of production optimization aiming at maximizing the NPV. We conducted a first optimization of the operational variables of the wells (injection/production flow rate and pressure) with common water injection, considering the economic scenario of the benchmark used. Next,

we performed the optimization of the same model, using EWI; in this case, variables of wells, the ion concentrations, and the interpolator were added as optimization parameters. Thus, it was possible to compare which injection method would yield the highest profit and what the optimized ion configuration would be.

As a tool for optimization, the original Fast Genetic Algorithm (SAMPAIO et al., 2015) was used, applied in this stage to maximize the NPV field. The best-trained network was coupled to the optimization, adding a step to the FGA code with the salinity concentration and interpolator ion as decision variables. This routine also extracted the original Kr curve from the corresponding model optimized, transforming it into Corey parameters and organizing with the chosen salinities, giving these data to the neural network "Net15_BR", which provided the new Kr curve. In general, this coupling was necessary to predict the new Kr curve at a given ionic concentration defined by the optimization process, inserting this curve in the corresponding model before the simulation stage.

2.5 Case Studies

2.5.1 Engineered Water Conventional Simulation Features

As previously mentioned, it is necessary to preset of the salinity composition of the formation water, mineralogic content, the geochemical reactions, and the modeling method to perform the simulation with EWI. Thus, to simplify the modeling method, we select the interpolator ion method and its salinity range (Tables 1 and 2).

Table 1: Parameters for modeling EWI in the simulator.

EWI Parameters for Simulator				
Kr Interpolation Begin (ppm)	Kr Interpolation End (ppm)	Sets of Inputs	Sor Reduction (Sor - EW/Sorw)	Krw Reduction (Kr - EW/Krw)
700	200	2	0.6	0.75

Source: Perform by Author.

Table 2: Ionic concentration of water injection and mineral percentual range.

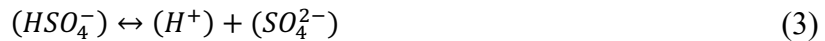
Formation Water Salinity (ppm)							Mineral Concentration (%)	
pH	Cl ⁻	SO ₄ ²⁻	Ca ²⁺	Mg ²⁺	HCO ₃ ⁻	Na ⁺	Calcite	Dolomite
7	17500	100	100	100	100	17500	0.5	0.5

Source: Perform by Author.

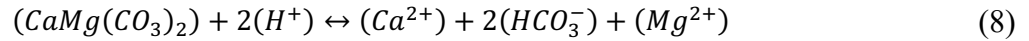
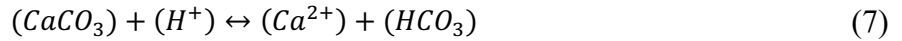
These settings were defined arbitrarily, as the formation water composition had about 35,000 ppm of total salinity, composed basically of Na⁺ and Cl⁻. For mineral concentrations, we set 50% dolomite and calcite, according to the pattern found in most carbonates.

Each template selected for constructing the database generated 15 new cases of EWI geochemical modeling, with random salinity ranging from 1000 to 9999 ppm and considering the same configurations on the formation water and mineralogical content shown above (Tables 1 and 2). In every 5 cases with EWI, the alteration in the potential interpolation ion (between SO₄²⁻, Mg²⁺, and Ca²⁺) was defined, increasing the diversity of ionic combinations and their corresponding effects. Finally, with all the 19 templates with 15 EWI random salinity cases created, we simulated these 285 samples and extracted the required data for the next step in the training network. With the data in Tables 1 and 2 kept the same for all tested models, changes in production are attributed exclusively to different ionic combinations. That allows the correlation between the new Kr data via Kr-Module with the corresponding salinity used in each model.

The fluid model was composed of seven components (Cl⁻, SO₄²⁻, Ca²⁺, Mg²⁺, HCO₃⁻, Na⁺, H⁺), and rock contained two minerals (Calcite and Dolomite). Four aqueous phase reactions to describe the ionic interactions in the geochemical simulation were included:



These reactions were selected, respecting the main interactions between the NaCl and the three potential ions. The mineral phase reactions that incorporate the Calcite and Dolomite dissolution and precipitation are shown below:



According to Dang et al. (2015), the difference between the composition of the in-situ and injected water disrupts the initial geochemical conditions, so the chemical equilibrium reactions calculate the behavior of these salts in each reservoir cell. On the other hand, the wettability alteration modeling occurs through shifting in the relative permeability curves, and the controller of this adjustment in the curves is the ion compositions obtained through these equilibrium reactions. Thus, this ionic balance in each cell allows a more precise adjustment in the relative permeability curves, considering the variation in salinity in different regions of the model.

2.5.2 Optimization Settings

At the optimization stage, a decision criterion was necessary for the algorithm to select an interpolator ion as an adjustable variable defining a chosen range of between 1 to 3, and the algorithm was specified as shown in Table 3.

Table 3: Range defined for the algorithm chosen between each interpolator ion.

Definition of Ion Interpolator	
SO ₄ ²⁻	Between 1 and 1.5
Ca ²⁺	Between 1.6 and 2.5
Mg ⁺	Between 2.6 and 3

Source: Perform by Author.

The algorithm thus selected the value within the range, and automatically transformed that number into the equivalent potential ion.

After the successful coupling of the neural network to the FGA, the initial parameters of the optimizations were configured (Table 4). We performed a series of tests, setting the maximum number of 200 individuals in the optimizations.

Table 4: Parameters for optimization with FGA.

Fast Genetic Algorithm Parameters	
Number of generations	20
Population size	10
Elite individuals	1
Crossover rate	0.8

Source: Perform by Author.

2.5.3 UNISIM-II Benchmark

The case study selected in this work was the UNISIM-II, developed by the Unisim group from Unicamp (CORREIA et al., 2015). The model structure combines the Brazilian Pre-salt and Ghawar fields, providing the description of an economic scenario as well. The dimension of this carbonate reservoir model is 5000x5000x150m and composed of 16 faults. Each grid cell has 50x50x1m, with a thin super-k zone. Further field information is:

- Depth of reservoir between 5,000 and 5,500m from the sea level;
- Initial reservoir pressure 560 kgf/cm²;
- Intermediate-wet relative permeability;
- Live oil viscosity to 1.14 cP;
- Reservoir temperature equal to 58.8°C.

The benchmark determines operational boundaries for injection and production wells (Table 5), used as upper and lower limits in the well optimization step.

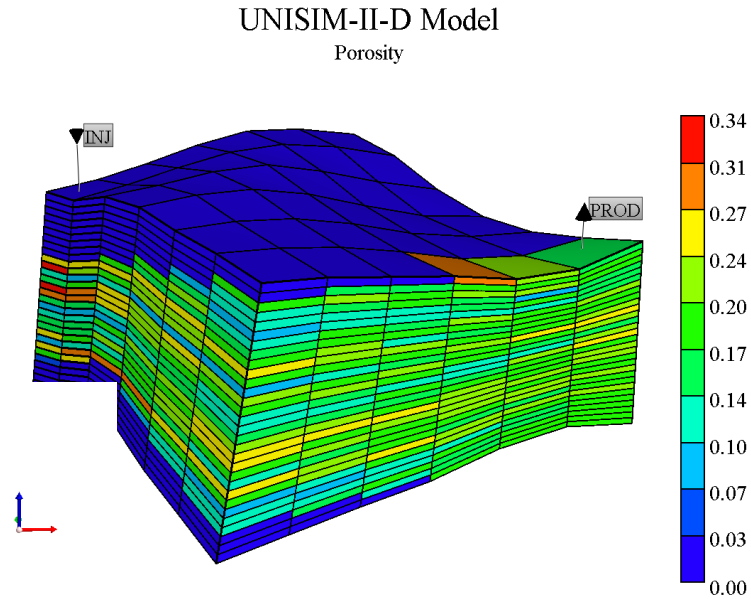
Table 5: Operational well conditions, adapted by Correia et al., (2015).

Type	Vertical Producer	Vertical Injection
Max. water rate (m³/day)	-	5000
Min. oil rate (m³/day)	20	-
Max. liquid rate (m³/day)	2000	-
BHP (kgf/cm²)	Min 190	Max 350

Source: Perform by Author.

To minimize the simulation time, we reduced the reservoir size selecting a section with 6x6x30 cells (Figure 8) chosen in a representative location, that preserves its architecture and behaviors. We also implemented one vertical injection well with a quarter of the area open to flow in the corner of this cut model, and a production well with the same condition in the opposite corner. The layout of the wells follows the injection pattern with a quarter of five-spot configuration, with a 450m distance between them.

Figure 8: Cut model from USINIM-II-D, showing the porosity parameter.



The deterministic approach of the benchmark used contains its economic scenario (Table 6), which updated the gas cost and price based on the U.S. natural gas price. Following the indications in the model description, we calculated the investment cost in the platform using the equation presented by Hayashi (2006) (Equation 3). We considered the maximum wells capacities of a quarter of the given description, adjusting this investment to the settings defined for the cut model.

$$INV_{PLAT} = 417 + (13.2 * Cp_o + 3.2 * Cpl + 3.2 * Cp_w + 3.2Ci_w + 0.1 * n_w) \quad (3)$$

Given that:

- INV_{PLAT} : Investment on the platform (USD millions);
- Cp_o : Oil processing capacity (1000 m³/day);
- Cpl : Liquid processing capacity (1000 m³/day);
- Cp_w : Water processing capacity (1000 m³/day);
- Ci_w : Water injection capacity (1000 m³/day);
- n_w : Well's number.

Table 6: Economic scenario used in the optimization study.

Variables	Values
Oil price	54.76 US\$/STB
Gas price	0.70 US\$/STB
Costs (US\$/stb)	
Oil production	10.952
Gas production	0.4675
Water Production	1.1
Engineered Water Injection	1.98
Water injection	1.1
Investments (US\$ millions)	
Drilling and Completion vert. well	22.8/m
Connection vertical well-platform	13.3
Platform	Equation 3

(1) PIS and COFINS are specific Brazilian taxes.

Source: Adapted from Correia et al. (2015).

2.6 Results and Discussion

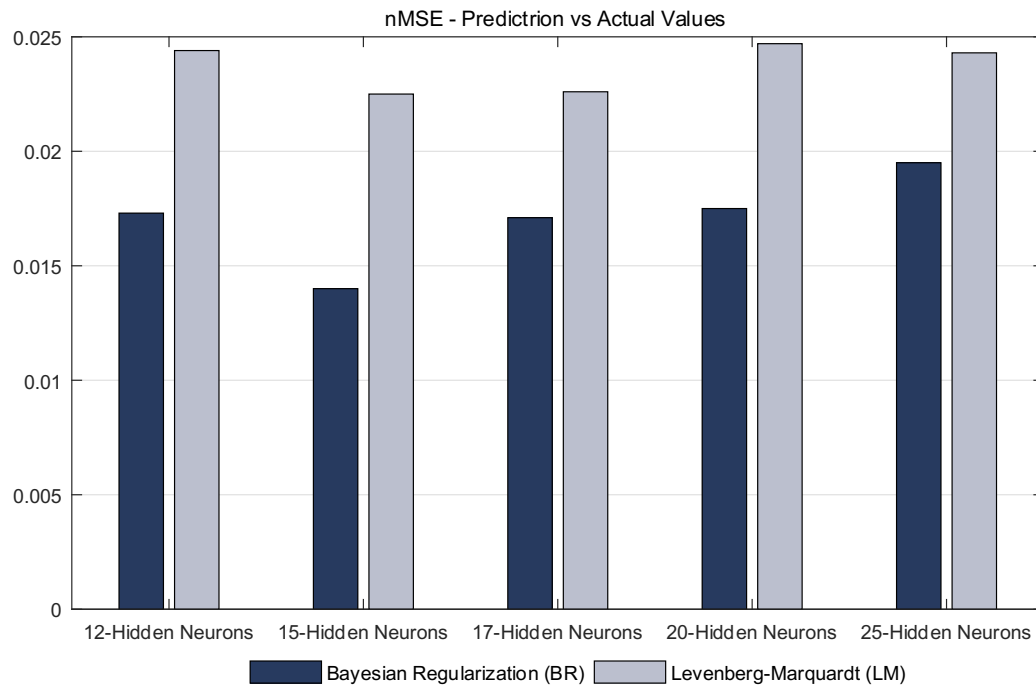
In this section, we divided the results into two parts. First, we approached the quality of neural network prediction based on statistical tools (nMSE). We then compared the optimization results, evaluating the final profit with the injection of seawater and EWI, the wells conditions, and the optimum salinity solution. We also optimized four cases of EWI varying only the cost of this engineered water injection, which showed its influence on the profits and on the optimized ion composition.

2.6.1 Validation of Network Predictions

We tested different neural network configurations to guarantee the best performance. We compared five sizes of hidden layers with two distinct training algorithms

(Figure 9). According to the theory, the training method of Bayesian Regularization (BR) is more indicated due to its data configuration, even so, we tested the training with the Levenberg-Marquardt (LM) algorithm to ensure that.

Figure 9: Comparison with the prediction performance network varying the number of hidden neurons and learning algorithms.



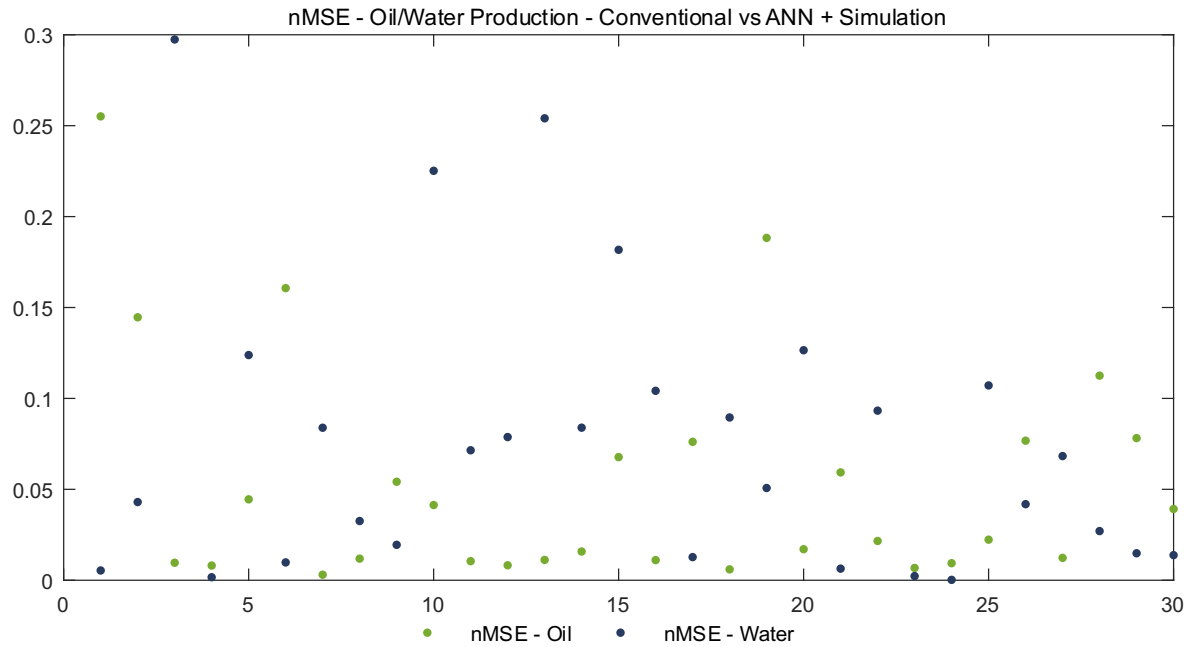
Source: Perform by Author.

In Figure 10, the comparison uses the data generated specifically for validating the networks already trained with the 30 cases of random salinity from the UNISIM-II model. Note that these data are not used in the training of the neural network, proving its ability to predict and to generalize through the normalized Mean Squared Error (nMSE). The nMSE shows that the closer to zero, the more similar the forecast result is than the expected value. Thus, based on nMSE, the neural network that obtains the best result is the one with 15 neurons in the hidden layer (Net15_BR). We noted that the variation between the nMSE with each training algorithm is not sharp, but this difference generates divergence in the production simulation because the Kr has high sensitivity in the software, making it essential to use the network with the best performance.

It was possible to confirm the benefits of using the BR network with the determination of relevance (ARD) and robust regularization (Figure 9). The absence of that in the LM algorithm impaired its training, which achieved high learning speed; but in these conditions, the regularization effort by BR is compensated with a better forecast.

The Net15_BR was coupled to the simulator to forecast Kr curves at a given salinity of the water injection, and we started to investigate the quality of this approach in production simulation. Thus, using the UNISIM-II model and its 30 test cases, we compared the production result between geochemical EWI modeling of GEM simulator and the ANN approach, following the same salinity compositions as the test models. The nMSE was applied to quantify the similarity in the oil and water production curves between these two schemes for EWI modeling (Figure 10). The comparison of results shows a satisfactory quality in the replacement of the geochemical modeling CMG package with the neural network, which was able to reproduce similar behaviors in the production simulation through only changes in Kr. The mean of the nMSE for the 30 cases compared in the analysis was mean-nMSE of oil equal to 0.0528 and mean-nMSE of water equal to 0.1189, with satisfactory results of the simulation performance coupling the ANN, enabling its use at the optimization stage.

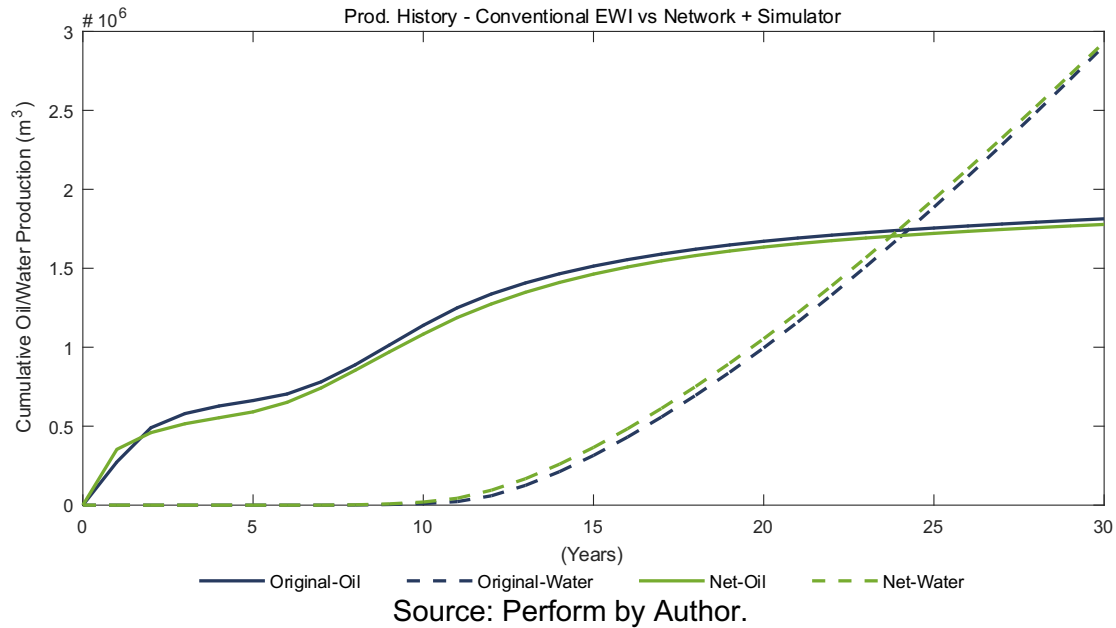
Figure 10: Normalized Mean Squared Error (nMSE) of Oil/Water Production between Conventional Simulation and Simulation with Net15_BR coupled.



Source: Perform by Author.

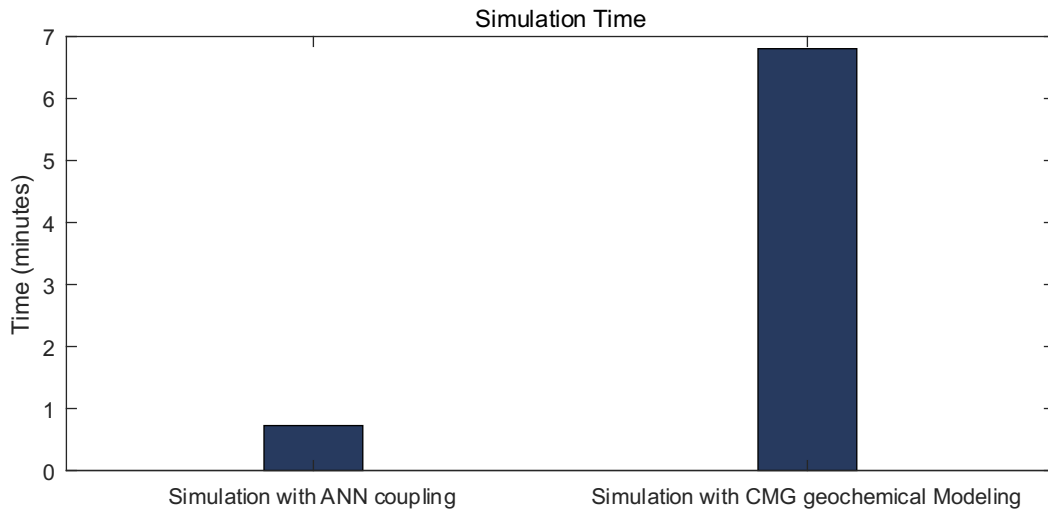
Figure 11 displays a plot referring to model 14, one of the cases with values closer to the average of the tested models. We plot with production histories generated between the compared methods, being possible to observe the quality that the ANN approach (in green) reproduces.

Figure 11: Simulation Results, comparing the traditional EW Simulation and Simulation with Net15_BR relative permeability results.



We also compared the aspect of simulation time (Figure 12), in which the ANN's predictive agility did not add more calculations to the numerical simulation, providing its simulation solution faster than conventional modeling. The software geochemical EWI modeling package adds calculation routines to predict the behavior of ion dissolution and adsorption rates, increasing the computational effort and the solution time. Therefore, the ANN application ensured similar results to the GEM modeling package with a significant time reduction.

Figure 12: Simulation time comparison between the ANN coupling solution and conventional geochemical modeling.



Source: Perform by Author.

2.7 Optimization Results

The optimization of UNISIM-II using seawater injection and EWI was performed, enabling the comparison of performance in oil recovery and its effects on the financial return on each injection project. The results are based on real costs and prices, but do not represent legitimate profitability; even so, they still allow a reliable comparison.

The economic evaluation description of the benchmark did not contain the EWI cost, so we define an increase of 25%, 75%, 300%, and 500% in relation to seawater injection cost. Thus, we performed four cases of EWI optimization, varying only the water injection price with salinity control, adding to the analysis the changes in ion composition generated by differences in its cost.

The results of the variables of wells, ionic concentration, the ion interpolator, and corresponding maximum NPV for each optimization case is displayed in the table below (Table 7). Notice the pressure of wells and flow conditions are similar in all the optimized cases, assigning the injection salinity in NPV changes. Also, three cases of EWI (25, 75 and 300%) had higher profits than the common water (seawater) injection, indicating that the advanced method is potentially more profitable considering a margin of up to 300% increase in the injection cost.

Table 7: Optimization results for each adjusted variable in the common water injection and Engineered Salinity.

Case	INJ- Rate m ³ /day	INJ- Press kPa	PRD- Rate m ³ /day	PRD- Press kPa	Ca ²⁺ (ppm)	SO ₄ ²⁻ (ppm)	Mg ²⁺ (ppm)	EW- mod	NPV (MMUS\$)	ΔNPV (MMUS\$)
Water	4988.29	33919.73	1996.66	17943.14	-	-	-	-	\$16.95	-
EW - 25	4866.87	33087.09	1961.96	17353.35	7127.23	5420.62	1033.83	3	\$66.57	\$49.62
EW- 75	4940.44	33591.59	1982.98	17710.71	7333.23	6627.23	1975.58	3	\$58.54	\$41.60
EW- 300	4975.48	33831.83	1992.99	17880.88	8931.33	8038.64	739.54	3	\$24.69	\$7.74
EW- 500	4898.4	33303.3	1970.97	17506.51	8715.52	8401.6	1661.66	3	\$8.22	-\$8.73

Source: Perform by Author.

When compared the results of accumulated production/injection fluids between the methods used (Table 8), the oil recovery increases by about 8.7% with EWI; the injected volumes are maintained close, and the water production is reduced by around 52%, saving this cost and improving the injection performance through ionic calibration. In sum, more oil was recovered with the same injection amount, and more water remained in the reservoir.

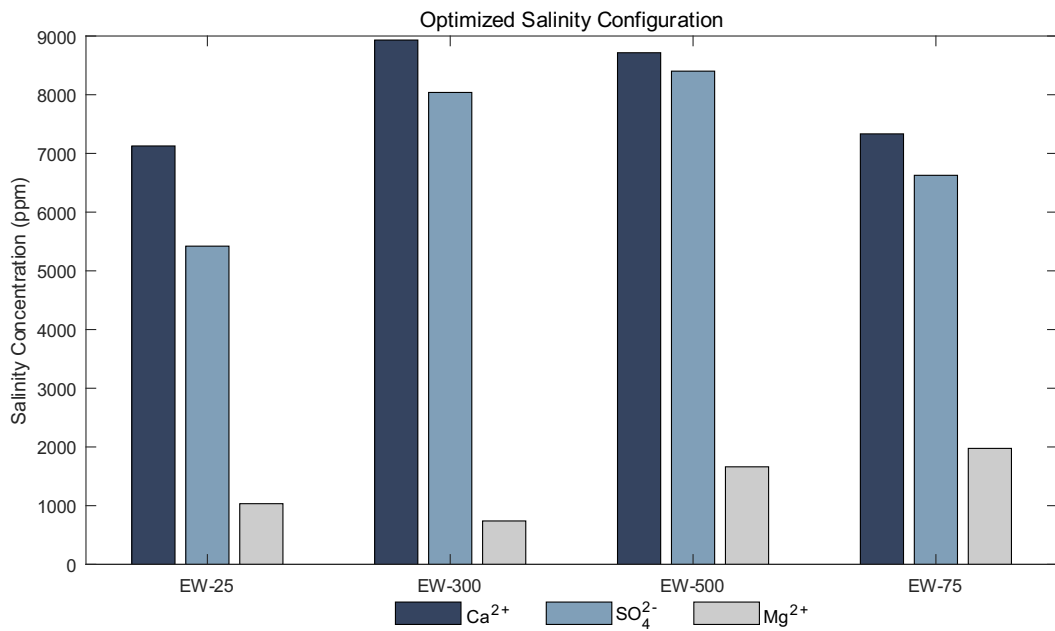
Table 8: Fluids production/Injection and oil recovery factor in the optimum cases.

Case	Oil Produced (10 ⁵ m ³)	Water Produced (10 ⁵ m ³)	Water Injection (10 ⁵ m ³)	Oil Recovery Factor (%)
Water	15.61	19.19	39.63	37.74
EW-25	19.66	9.45	36.38	47.53
EW-75	19.58	8.61	35.66	45.35
EW-300	18.30	10.64	35.25	44.22
EW-500	19.06	7.96	34.59	46.07

Source: Perform by Author.

The optimized salinities (Figure 13) show the sulfate and calcium with higher concentrations, increased their quantities with rising cost. All four EWI cases show Ca²⁺ as the interpolator ion (Table 7), but this does not minimize the effect of the other salts, which in this application changes with their different combinations, considering multiple influences between them.

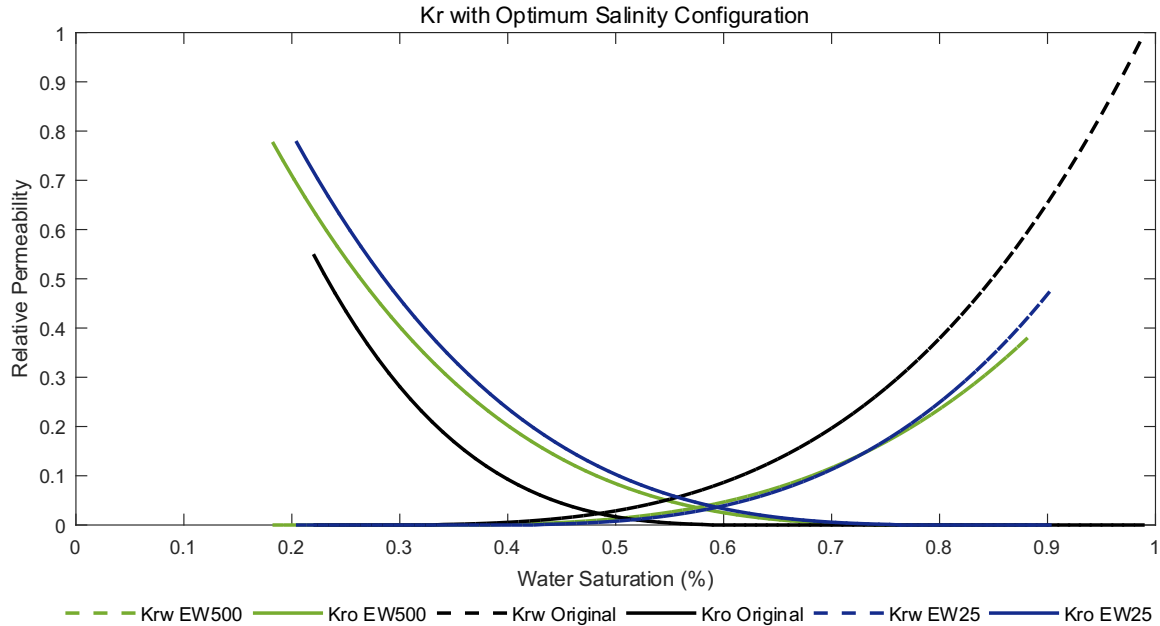
Figure 13: Ionic concentration of water injection obtained by the optimization process.



Source: Perform by Author.

This step shows the optimized concentrations are not low, reinforcing that to improve the projected water injection technology requires exploration with a higher range of ion concentrations considering their technical and economic viability. As pointed by Adegbite and Al-Shalabi (2020), the low salinity levels bring benefits in most injection cases. On the other hand, its optimization can converge to a more concentrated use of some ions, showing a greater versatility of the EWI technique.

Figure 14: Relative permeability of Engineered Water Optimized versus Normal relative permeability.



Source: Perform by Author.

Finally, we plot the relative permeability curves of the original case, EW-25, and EW-500 (Figure 14), analyzing the changes that the ionic compositions produced. We observed an increase in the Kr-Oil curve values and a reduction in Kr-Water with the proposed ionic concentrations when compared with the original case. The EWI has the potential to increase the difference between connate and critical water saturation due to changes in the oil flow. The Kr-Oil with EWI had lower saturation points of connate water than the original case, reinforcing this expected effect by the injection method. An increase occurs at the endpoint on the Kr-Oil curve with EWI, indicating a higher final water saturation, with a consequent reduction in residual oil saturation. Analyzing the Figure 14 based on the changes in S_{or} and the shape of the Kr-Oil curve, we noticed an oil mobility modification by the optimized ionic injection, which resulted in a direct impact on the behavior of oil production and on the injection/production water. These comparisons indicate a change in the natural wettability of the rock preferential to water (more water-wet), corroborating the theories approached for the injection method.

2.8 Conclusions

In this article, we developed a feedforward neural network that performed changes in the relative permeability data given an ionic condition, having the potential to reproduce the same effects in the numerical simulation, considering the EWI geochemical modeling of the CMG software. The development of ANN underwent practical tests to define its configurations, such as the number of neurons in the hidden layer and the choice of the training algorithm, based on the forecast quality (nMSE around 0.0137) that reached the best results with Net15_BR. At this stage, several theoretical concepts were applied, showing that the nature and amount of data used require practical tests to guarantee the best performance of the tool. When coupling the neural network trained in the simulation software, we compared its numerical simulation with the results from the conventional method of EWI modeling, ensuring a reliable outcome with this new modeling strategy. We also compared the simulation time between these methods, in which the neural network is fast to predict the necessary adjustments to K_r , not increasing new calculations to the production simulation, unlike geochemical modeling, thus reducing the simulation time by an average of 90%. The UNISIM-II benchmark and its economic scenario provided the optimization of seawater injection and EWI. At this step, the NPV of the field was maximized using the flow and pressure conditions of the wells and the salinity of the water injection (in the case with EWI) as adjustable variables. The results showed that the injection with EWI had a positive effect on the final production profit, with an increase of 49.62 million dollars (without considering additional Capex due to EWI implementation). We compared the accumulated production, in which the projected water injection increased oil recovery by about 8.7% with the same injected amount and reduced the accumulated water production by around 52%, compared to the seawater injection. EWI avoided excessive water production and increased the volume of oil recovered. The EWI-500 (500% base value increase) case is the only that has NPV less than seawater injection; this guarantees the application of the advanced method with a high-cost margin. We emphasize that although the economic attributes used are reliable, they do not represent a real production scenario, which certainly has other investments and revenues considered. The optimization results converged to use higher concentrations of sulfate

and calcium, showing the importance of investigating the injection with a higher salinity range, but respecting the technical or economic limits. The increase in the K_r of the oil, reduction in the K_r of the water, and a decrease in the residual oil saturation confirmed the K_r changes to more water-wet conditions. These results in K_r corroborate other studies applied to the EWI method, reinforcing the advantages of controlling salinity for managing fluids displacement in the reservoir.

2.9 ACKNOWLEDGMENTS

The authors would like to thank LASG (Laboratory of Petroleum Reservoir Simulation and Management), InTRA (Integrated Technology for Rock and Fluid Analysis) and Escola Politécnica of the Universidade de Sao Paulo. This work was conducted with the ongoing Project registered as "Projeto de Molhabilidade e Propriedades Petrofísicas de Rochas Carbonáticas e sua Relação com a Recuperação de Hidrocarbonetos" (USP/Petrobras/ANP) funded by Petrobras, under the ANP R&D levy as "Compromisso de Investimentos com Pesquisa e Desenvolvimento". The authors would also like to thank FAPESP (the State of São Paulo Research Foundation), and CMG[®] and MATLAB[®] for software licenses.

CHAPTER 3 - HYBRID MACHINE LEARNING TO MODELING THE RELATIVE PERMEABILITY CHANGES IN CARBONATE RESERVOIRS UNDER ENGINEERED WATER INJECTION

Abstract

Advanced production methods usage complex fluid interaction mechanisms to provide benefits in their use. Thus, its modeling is always complicated to incorporate all the effects with accuracy and agility. These conditions are ideal for Machine Learning (ML) applications that are fundamentally data-driven. In general, ML tools seek to establish a simple relationship between variables to learn the behavior of a target and predict it. Therefore, we couple a Hybrid Machine Learning (HML) solution to predict the petrophysical behaviors during the Engineered Water Injection (EWI). The hybrid methodology uses two machine learning algorithms (K-Means and Artificial Neural Network), performing in the first step a classification of the original input permeability and then predicting the new relative permeabilities with different injection salinities. This pipeline to model the injection with HML is validated first by comparing the actual and predicted permeabilities curves. Then, we evaluate the solution in production simulation, comparing that outcome with conventional geochemical modeling. Finally, we execute an optimization with common water injection and EWI (with HML modeling) to maximize the Net Present Value (NPV) of a case study. Like so, that optimization validates the HML in interactive predictions, also comparing the injection methods performance. These tests present a better option to use the advanced method, which increases the oil production (around 7.3%) and dramatically decreases the water injected and produced (-28% e - 40%), being more profitable even which increasing its injection price.

3.1 INTRODUCTION

Artificial Intelligence (AI) technologies are increasing in applications in the oil and gas industry due to the challenges of dealing with high volumes of data (BANGERT, 2021; HAJIZADEH, 2019). One of these technologies, Machine Learning (ML), has the advantage of processing high amounts of data efficiently, bringing reliable solutions to

different problems. According to Hajizadeh (2019), the number of papers on the Machine Learning (ML) topic, has been growing exponentially in current years. Also, the current digital transformation acts as a catalyst for the comprehensive usage of these techniques (EVANS, 2019).

The application of reservoir modeling and simulation requires a numerical approach based on physical laws, such as mass conservation, thermodynamics, hydraulic diffusivity, etc. Although being considered a reliable tool, its results only in an estimation of the actual measured data. Indeed, some physical phenomena have a nonlinear behavior, being complex to model. On the other hand, an alternative based on the relationship between the data is more advantageous in some applications, like in the reservoir petrophysical behaviors case (LIU et al., 2019; MASOUDI et al., 2020; MOHAGHEGH and AMERI, 1995).

In addition, the inclusion of physicochemical interactions in the simulation process (such as Enhanced Oil Recovery - EOR - injections) lead to even harder numerical estimations. In this case, an alternative is use laboratory data in the numerical model, but this ties the solution to specific tools, leaving reproducibility limited to the process of generating laboratory data (MOSALLANEZHAD; KALANTARIASL, 2021). The EOR engineered water injection (EWI) technique that controls the salinity of the injected water to increase the volume of recovered oil is an example of injection with a complex geochemical background (KORRANI et al., 2014). This ionic control achieves polar interactions with the rock altering its natural wettability properties and facilitating fluid permeability (AUSTAD et al., 2007; ROSTAMI et al., 2019; SULEIMANOV et al., 2018).

The geochemical behavior that occurs with injection adds more complexity to its numerical solution. Understanding these limitations, we proposed to use an approach through a hybrid ML solution. Which a way, can learn the relationship between the variables of relative permeability, salinity (formation and injection), and mineralogy, becoming able to incorporate in the changes of K_r related to the injection method.

To simplify the modeling of engineered water injection, we implemented a solution with two complementary machine learning tools (K-Means and Artificial Neural Networks) to establish a relationship among salinity, relative permeability, and mineralogical content. Thus, we have a reliable approach with ML to reproduce the production simulation similar to conventional geochemical modeling. In this case, we initially use a clustering method to classify the original relative permeability (K_r), and in sequence, with a given injection salinity, is predict a new K_r curve. The use of these two specific ML tools defines as Hybrid Machine Learning (HML).

Finally, we tested the quality of the EWI modeling pipeline with Hybrid ML in an iterative optimization process. Thus, we selected a benchmark, Unisim-II, applying two injection processes: (i) with common water and (ii) engineered water. Using the economic scenario proposed in the benchmark, we maximized the Net Present Value (NPV) with 30 years of production in both cases, increasing only the cost of the engineered water by 35%. In these tests, the EW injection had the highest NPV, increasing the final profit by approximately 39%, compared with the other injection. This performance is due to an increase in oil recovery of 7.3% and the reduction in water injection and production in 28.5% and 40%, respectively.

3.2 METHODOLOGY

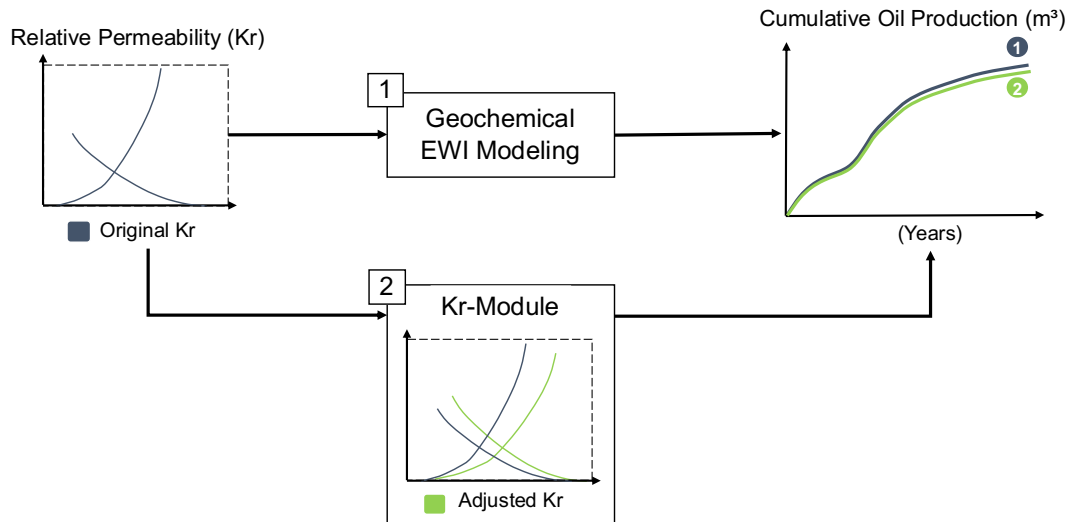
3.2.1 Data Collection

To build the database, we selected 30 templates from CMG's collection. Based on by SPE solution problems, these synthetic templates were simulated 50 times with the EWI method. Each geochemical modeling was performed randomly, keeping the characteristics of each case to ensure the results generalization. This synthetic data generation strategy by simulation took a data generation time of approximately one month to complete. Finally, with a total of 1500 simulated cases, we started the phase of structuring and cleaning the dataset. We adapted the methodology using templates to generate synthetic EWI data from Reginato et al. (2021). However, we added the variables of formation water salinity and mineralogical content in the initial geochemical modeling.

3.2.2 KrModule Procedure

After the simulation of synthetic cases, we use the KrModule algorithm to obtain the new relative permeability. This module works by recursively adjusting the Kr of a model with common waterflooding until yield results like the corresponding case with EWI (Figure 15). KrModule is a solution developed by Reginato et al. (2021) and adapted for this work. Here we replace the algorithm that minimizes the error between the production curves to the particle swarm optimization (PSO), which previously used the genetic algorithm (GA).

Figure 15: KrModule Schema.



Source: REGINATO et al. (2021).

Particle Swarm Optimization (PSO) is a method that works by improving a set of candidates (or particles) moving in the exploratory space through a velocity and position. At each iteration, all particles are readjusted by "moving" in the direction of the current best case.

At the end of the module application, we generate the new relative permeability that translates the effects of EWI in the simulation. Thus, we structured the dataset as follows:

Input:

- Kr original;
- Injection salinity concentration;
- Formation salinity concentration;
- Mineralogy.

Output:

- Kr adjusted.

In order to improve the network training performance by avoiding repeated data, we transform the relative permeability curves in the parameters of Brooks and Corey's (1984) equations (Equations 4 and 5).

$$k_{ro} = k_{rocw} \left(\frac{1 - S_w - S_{or}}{1 - S_{cw} - S_{or}} \right)^{no} \quad (4)$$

$$k_{rw} = k_{rwor} \left(\frac{S_w - S_{wcrit}}{1 - S_{wcrit} - S_{or}} \right)^{nw} \quad (5)$$

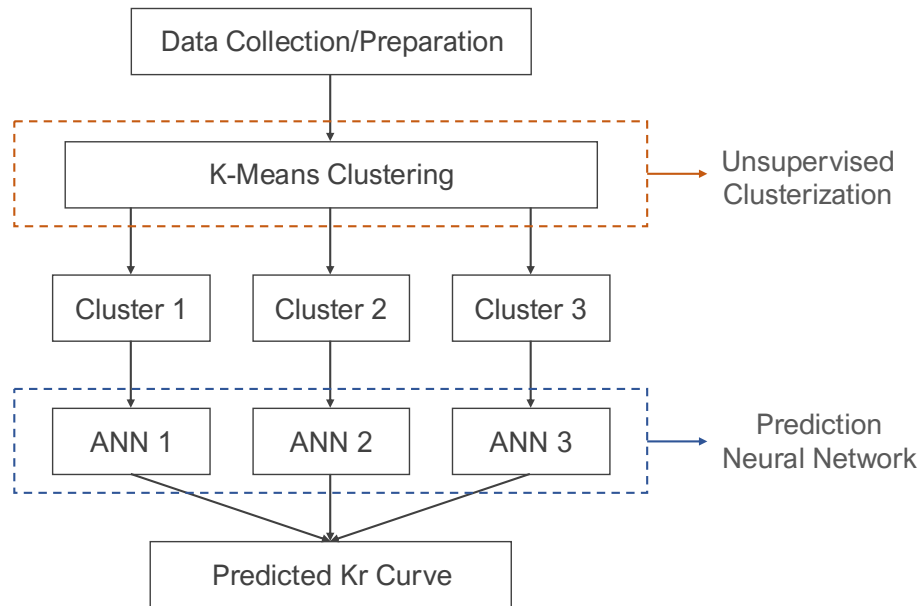
Equation 4: Oil Relative permeability; Equation 5: Water Relative permeability.

3.2.3 Hybrid Machine Learning Method

The main feature of the HML method is the association of two different ML algorithms. In the first step, we used an unsupervised clustering process, the K-Means algorithm from the Scikit-learn framework. The K-Means method groups the dataset by following the similarity pattern. It is also interesting that it does not use output labels, leaving only the training to find these relationships. For this step, we set the number of clusters equal to 3 based on the number of wettability types, keeping other hyperparameters with the algorithm's default settings. We also use only Kr original as input data. Thus, this clustering focused on 3 possible groups by input Kr.

Then, the complete data frame is divided into 3 parts following the labels assigned in the clustering phase. In this stage, we selected the artificial neural networks (ANNs) of the Multi-Layer Perceptron (MPL) type also from Scikit-learn, being able to make a performance comparison with the solution proposed by Reginato et al. (2021). Three of this ANN was trained using one of the three new corresponding datasets (Figure 16). These ANNs are structures of interconnected nodes (neurons), which learn basically by defining a pattern between the input and output data ideal for forecasting applications (MALEKIAN and CHITSAZ, 2021).

Figure 16: ML Hybrid method overview.



Source: Perform by Author.

The data set is subjected a standardization process before training with ANNs. We employed a mathematical transformation known as Standard Scaler that seeks to center the mean of the data at zero and balance the standard deviation in the same order. This solves the problem data sets with very discrepant feature scales, which if is not equalized, during the training the variables with high variance end up overlap the objective function and harms the training performance. The formula below summarizes the transformation process:

$$Z = \frac{X - \mu}{\sigma} \quad (6)$$

Equation 6: Standard Scaler Transformation.

The neural networks have undergone adjustments of their hyperparameters to improve validation results. We used a model selection approach (Grid Search Cross Validation) that systematically tests combinations of ANN configuration, calculating a score for each test. Thus, we were able to rank the results with the best prediction performance using the normalized mean squared error (nMSE) metric, selecting the best case for each ANN. In this process, the variables explored were:

- Hidden layer size: from 5 to 25 neurons;
- Activation function: logistic or tanh;
- Solver: lbfgs, sgd or adam;
- Learning rate: constant, invscaling, or adaptive.

The configuration and training of the K-Means model and the neural networks were completed. Then, the HML was ready to be engaged in the case study optimization process.

3.2.4 EWI and Water Optimization

The optimization process used has as an objective function of the Net Present Value (NPV) maximization. Thus, to promote a comparative approach, we performed two optimizations, with normal water and EWI. For the NPV calculation, we adapted the economic scenario from the case study.

The operating well parameters (flow rate and pressure) were the optimized variables. However, in the case of EWI, the salt concentrations of the injected water were added. Therefore, we had:

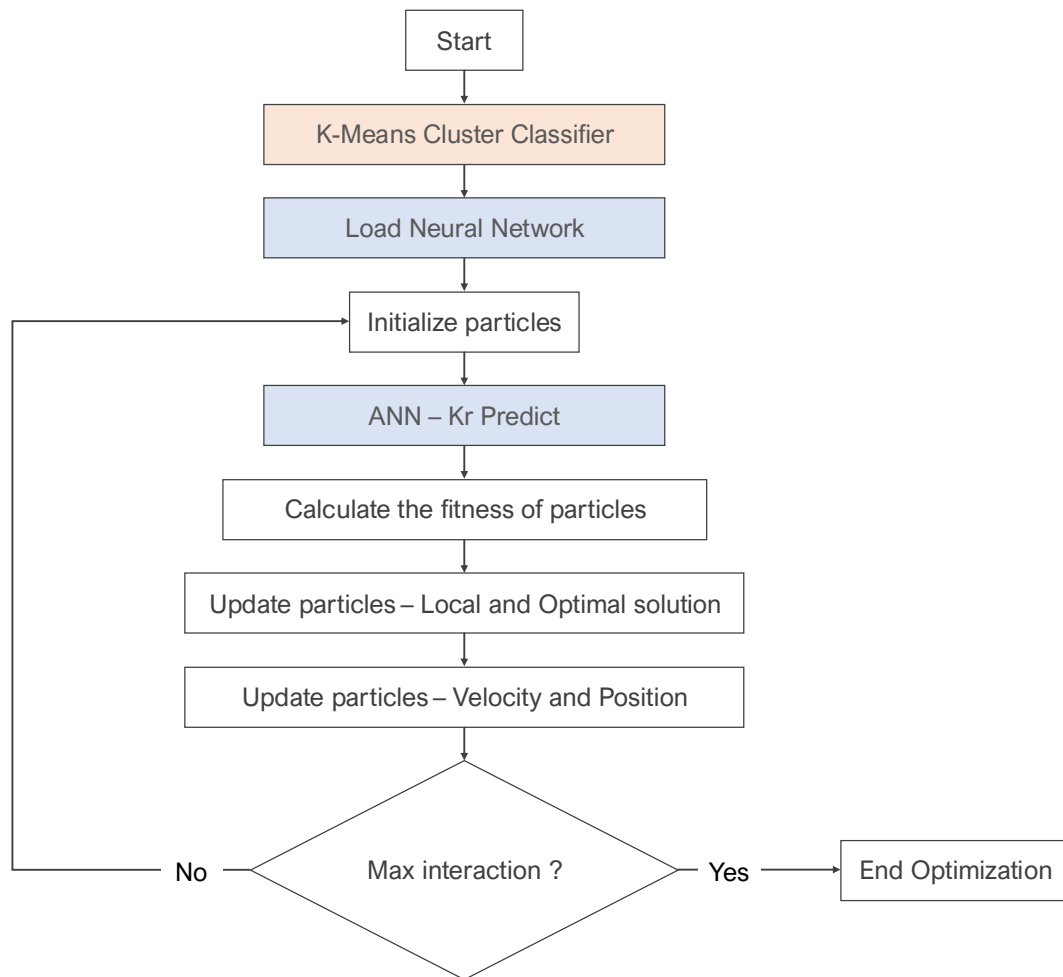
- Production Rate;
- Production Pressure;
- Injection Rate;

- Injection Pressure;
- Salinity concentrations (Na, Cl, SO₄, Ca, and Mg), just in the EWI scenario.

Particle swarm optimization (PSO) was chosen considering its simple implementation, fast convergence, and ideal for continuous space formulation problems. It is also a metaheuristic method, which avoids premature convergence to local minima.

At this stage, we had combined the HML to the optimization in the case of EWI, performing it in two steps. First, the K-Means model identified the relative permeability group (or label). Then, the neural network corresponding to the group was loaded. The neural network used the salinity set at each iteration with the original Kr to predict the new curve (Figure 17).

Figure 17: PSO with HML coupling workflow.



Source: Perform by Author.

3.3 CASE STUDY

3.3.1 UNISIM-II Benchmark

For the project, we selected the benchmark based on a field in the Brazilian Pre-Salt. The Unisim-II was developed by the Unisim research group (from Unicamp). This case study's structure combines data from the Ghawar field, dimensions of 5000 x 5000 x 150m, with 16 faults and a Super-K zone (CORREIA et al., 2015).

The production system defined in this model gives the injectors and producers operating ranges. That operational limits were used in the optimization phase (Table 9).

Table 9: Wells operational conditions, adapted by Correia et al., (2015).

Type	Vertical Producer	Vertical Injection
Max. water rate (m^3/day)	-	5000
Min. oil rate (m^3/day)	20	-
Max. liquid rate (m^3/day)	2000	-
BHP (kgf/cm^2)	Min 190	Max 350

Source: Perform by Author.

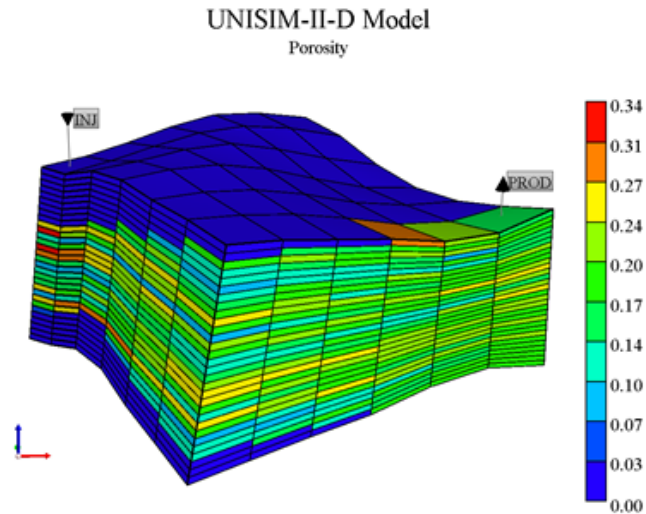
For better performance, we used a reduced model of Unisim-II, the same one used for Reginato et al. (2021). This part of the model has 6x6x30 cells in a representative field location. Following Reginato et al. (2021), the well configuration uses producer and injector wells in opposite corners of the model (one quarter of five-spot). Also, the economic scenario is adapted for the proportions of the benchmark cut fraction (Table 11).

Table 10: Economic scenario for reduced model (Reginato et al., 2021).

Variables	Values
Oil price	54.76 US\$/STB
Gas price	0.70 US\$/STB
Costs (US\$/stb)	
Oil production	10.952
Gas production	0.4675
Water Production	1.1
Engineered Water Injection	1.98
Water injection	1.1
Investments (US\$ millions)	
Drilling and Completion vert. well	22.8/m
Connection vertical well-platform	13.3
Platform	Equation

Source: Perform by Author.

Figure 18: Reduced Unisim-II model.



Source: Perform by Author.

For the advanced injection with engineered water, we assumed a saline composition of the formation and mineralogy. The benchmark is based in two carbonate reservoirs then the mineralogy was 50% calcite and 50% dolomite, the most abundant minerals in this type of rock. For the ionic configuration of the formation water, we decided on 35000 ppm of NaCl, 200 ppm of sulfate (SO_4^{2-}) and magnesium (Mg^{2+}), and 1000 ppm

of calcium (Ca^{2+}). The benchmark does not have these available data, so we defined these variables to proceed with the study.

3.3.2 KrModule PSO Parameters

The settings of the optimization algorithm used in the KrModule are shown below:

Table 11: PSO in KrModule Configuration.

PSO Features	
n particles	10
n interactions	12
K	1
φ_1	2.05
φ_2	2.05
wdamp	1
chi	Equation

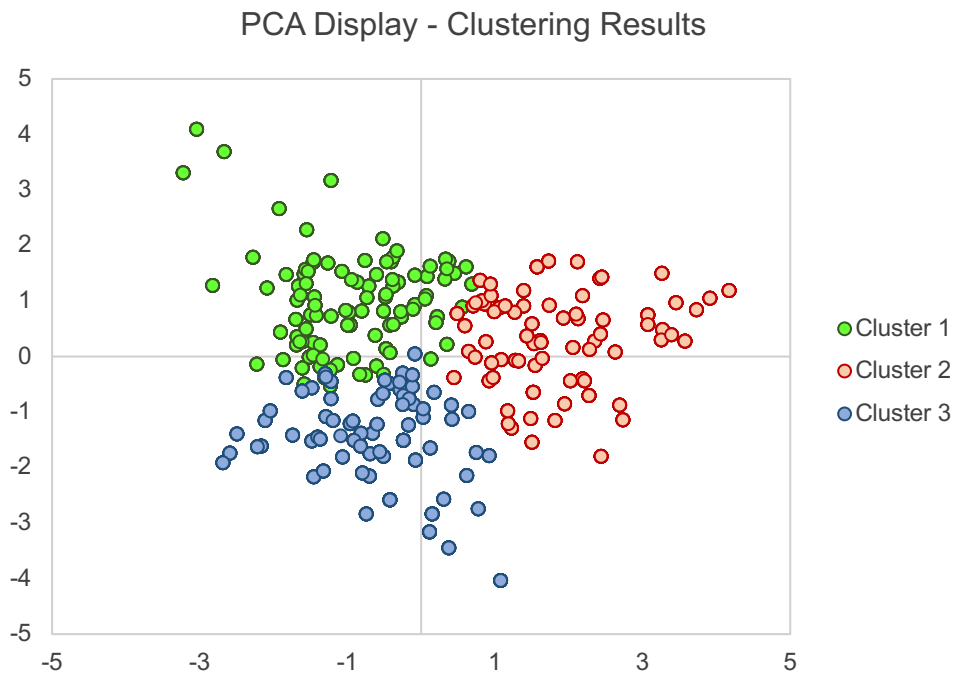
Source: Perform by Author.

3.4 RESULTS AND DISCUSSION

3.4.1 K-Means Clusterization Results

Initially, we obtained the classification between the three groups for each relative permeability defined via the K-Means. Then, we use an orthogonal transformation method (principal component analysis - PCA) to reduce the dimensionality of features. This widely used method transports the original parameters to a new orthogonal space, further reducing and simplifying the set. We applied the reduction from 8 to 3 components, one of them being the original labels of each cluster. Thus, we enable a 2D visualization (Figure 19) to incorporate the relevance of each reduced feature.

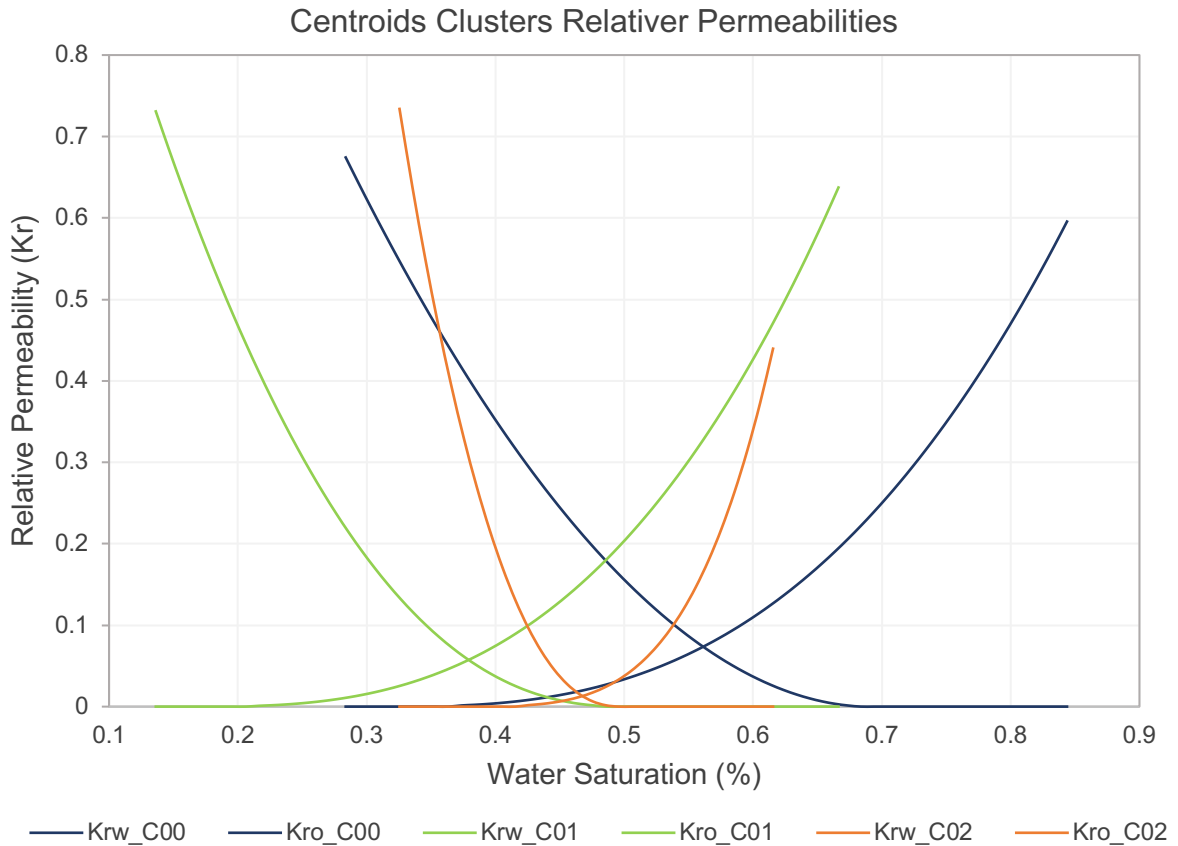
Figure 19: PCA plot segmented by clusters.



Source: Perform by Author.

Based on the plot, we noticed that the clusters are not well defined in the distribution, indicating that there is no significant clustering among the data. However, it was possible to generate a classification pattern by similarity. Thus, we observed the characteristics of each cluster through their respective centroids. We compared this sample central of the clusters (Figure 20) to analyze the characteristics belonging to each of them.

Figure 20: Centroids Clusters as Relative Permeability.



Source: Perform by Author.

We note here characteristics that we sought to segment at the beginning of the clustering process. The choice of 3 clusters in this step was not random. We use quantities of options for qualitative types of wettability: oil-wet, water-wet, and intermediate wet, following other applications with defines that wettability analysis by the relative permeability curve shapes (CRAIG, 1971; MIRZAEI-PAIAMAN, 2021).

Through clustering centroids, we see these features that define different wettability as Craig's method (CRAIG, 1971), grouped by the algorithm independently. Cluster 00 (in blue) has the most water wettability characteristics of all, with the intersection point of the K_r curves greater than 0.5 of S_w (second Craig's rule), lower residual oil saturation (approx. 0.67 S_w), and oil permeability curve with lower angulation level, which means, that oil permeability has slower reduction as S_w increases. Cluster 01 (in green), which

has a residual oil saturation (S_{or}) below 0.5 S_w , Kr-Oil curve with a large slope, and the beginning of water mobility already at low saturation (S_w at 0.25). For the class of intermediates, we have cluster 02, with characteristics between the two cases, but with the Kr-Oil starting point higher than Kr-Water and the two curves with the highest slopes.

3.4.2 Neural Network Results

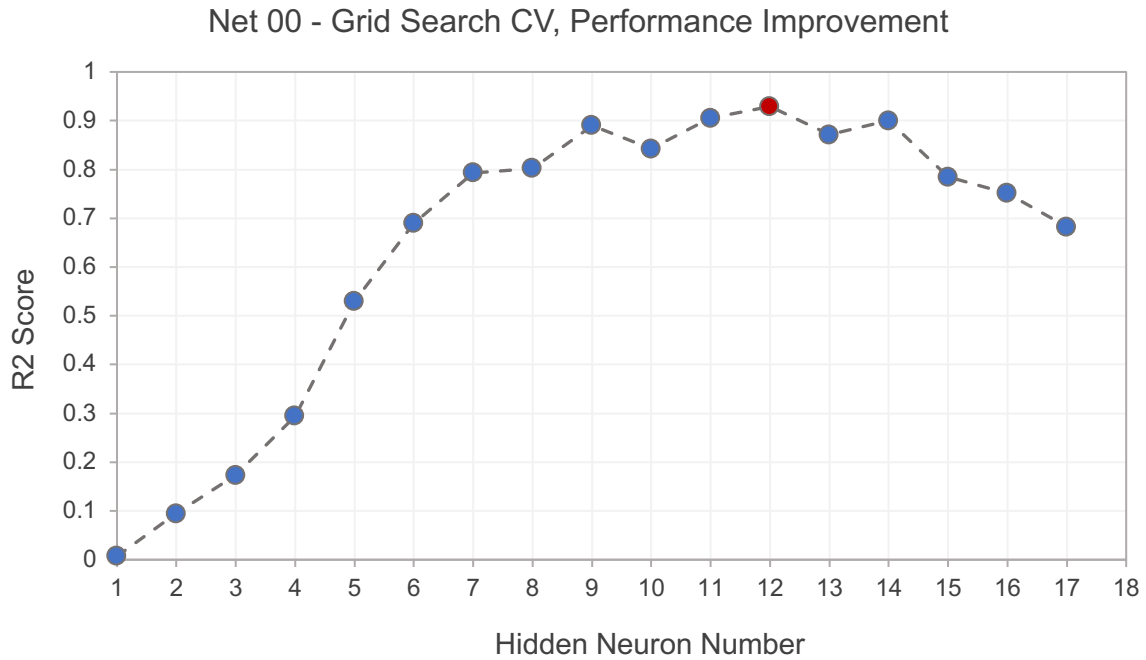
The neural net training uses the cross-validation method. Thus, we set 70% of the data for training, 15% for testing, and 15% for validation. Their hyperparameters achieve through grid search exploration (Table 12). In the end, we observe that the optimum net configurations did not present very expressive differences, but its application increased in all cases the performance of the predictions (Figure 21). This optimization application with systematic testing of neural network configurations ensures reliability in its performance. That is different from the Reginato et al. (2021) validation, which tested two learning algorithms on a smaller range of neurons in the hidden layer.

Table 12: Grid Search CV final optimization in each case.

Hyperparameter	Net 00	Net 01	Net 02
Hidden layer size	12	10	11
Activation	Logistic	tanh	logistic
Solver	lbfgs	lbfgs	lbfgs
Learning rate	adaptive	adaptive	adaptive

Source: Perform by Author.

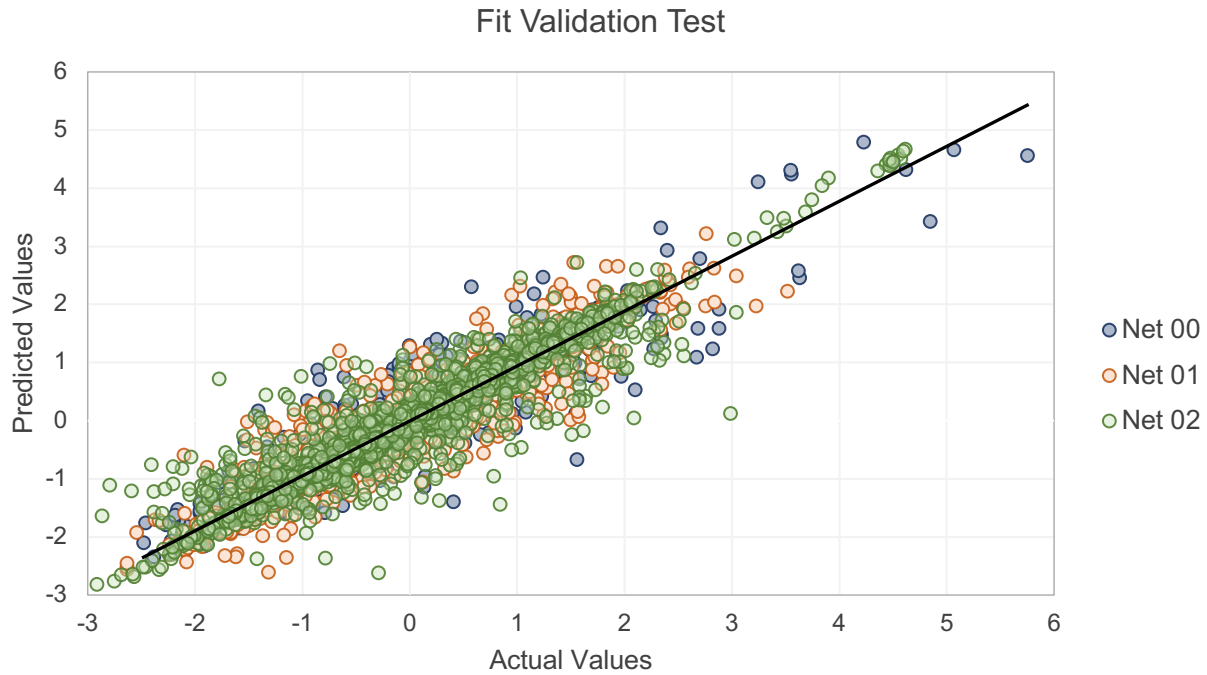
Figure 21: Net 00 R2 score vs hidden layers number using grid search CV.



Source: Perform by Author.

Next, using the validation fraction of the data, we compare the actual values with the predicted ones. Through a cross-plot (Figure 23), it is possible to observe the distribution of the three cases approaching the expected diagonal linear regression. We confirm the predictions by the R^2 score between the actual and forecast values, which were 0.929, 0.872, and 0.897.

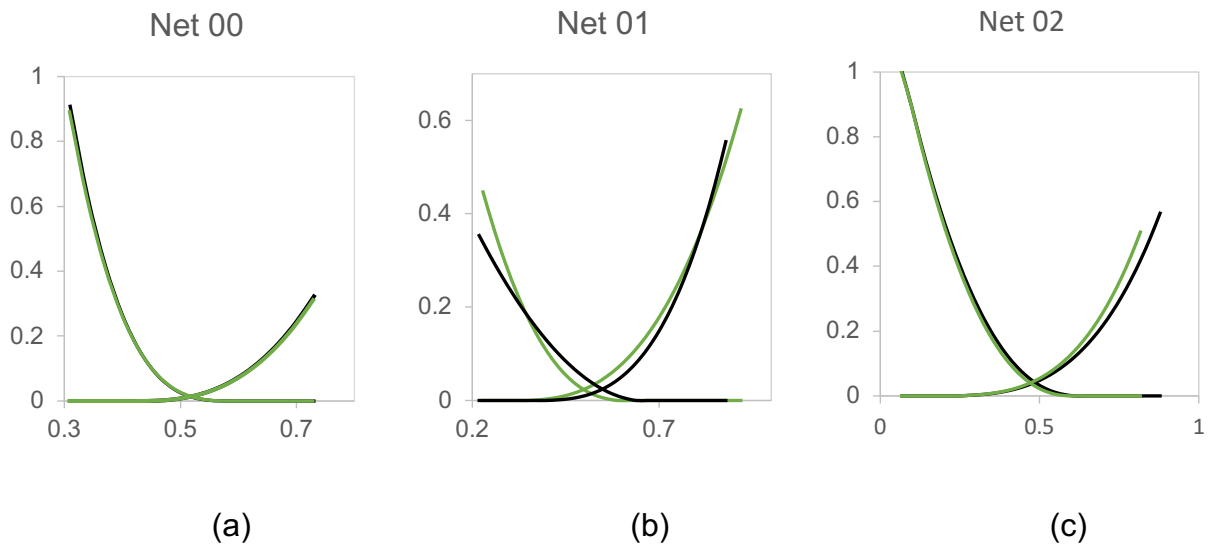
Figure 22: Cross-plot predicted vs actual values.



Source: Perform by Author.

We also selected three random Kr cases from the validation to compare the shape of the forecasted curves by the networks and evaluate their quality.

Figure 23 (a, b, and c): Comparison of Kr-Curve predicted by each network (green) and the actual curves (black).



Source: Perform by Author.

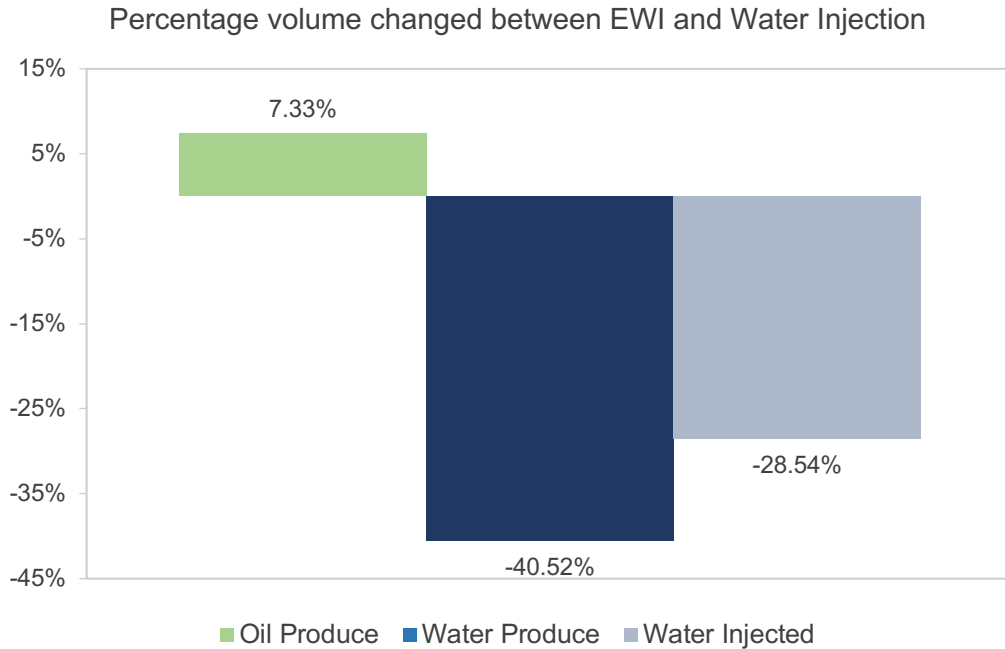
These plots confirm that the Network with the highest R^2 score provides an accurate fit of the curves. Nevertheless, the other networks also show well results when comparing the shape of the curves. Thus, it is possible to confirm the neural network application reliability with their results. The R^2 score of the ML approach performed by Reginato et al. (2021) is higher in absolute values (above 90%). But the current approach considers more training variables, enriching the behavior of K_r for the neural network to predict.

3.4.3 Optimizations

At this stage, we perform two optimization processes: (i) Unisim-II 6x6 with original water injection; and (ii) Unisim-II 6x6 with EWI. However, in the case of EOR, we increase by 25% the cost of injected water.

In the optimization with common water, the best case ended up with NPV equal to MM US \$18.21 in a 30-year production period, with an oil recovery factor equal 38%. In this case, it is worth noting that the volume of water produced is 6x highest than the volume of oil (Table 13). Compared to the results of the EWI case, there was not a very high increase in oil recovery but a significant reduction in production and water injection volumes (-28.5% and -40.5%). These changes promote a 45.3% increase in the final NPV result with the advanced method (approximately MM \$47.8).

Figure 24: Percent volume of fluids.



Source: Perform by Author.

Table 13: Fluids production, recovery factor, and final VPL from optimum cases.

	Oil Produce (10 ⁵ m ³)	Water Produce (10 ⁵ m ³)	Water Injected (10 ⁵ m ³)	Oil Recovery Factor (%)	Final VPL (MMUS)
Water	15.72	15.35	40.03	38.01	\$ 18.21
EWI	16.88	9.13	28.60	41.4	\$ 26.45

Source: Perform by Author.

The optimized wells variables in the two cases showed a convergence. The injection flow rate for the common water case is lower to control the injection volume/production of water that is very high.

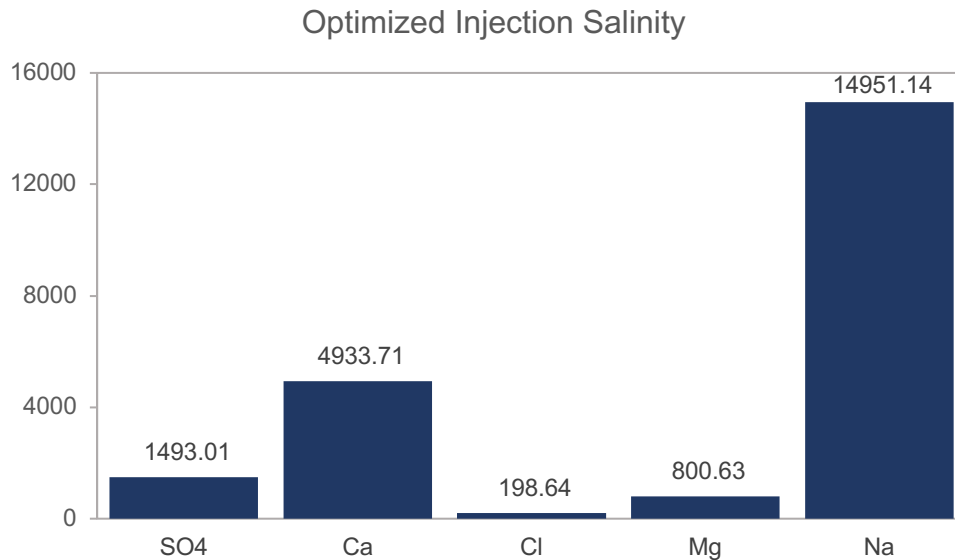
Table 14: Optimized variables results.

Inj Rate (m ³ /day)	Inj Pres kPa	Prd Rate (m ³ /day)	Prd Press kPa	SO ₄ ²⁻ (PPM)	Ca ²⁺ (PPM)	Cl ⁻ (PPM)	Mg ²⁺ (PPM)	Na ⁺ (PPM)
2,091.66	33,256.36	1,994.50	996.73					
2,878.92	33,565.98	1,995.80	989.79	1,493.01	4,933.71	198.64	800.63	14,951.14

Source: Perform by Author.

The optimum salt solution had 22,575 ppm in total, with more than half composed of sodium. The sulfate concentration is increased compared to the standard saline solution. This ion is relevant for promoting the geochemical iterations of wettability reversal, so this increase in concentration was expected for the final Kr adjustment to go to a higher water wettability condition.

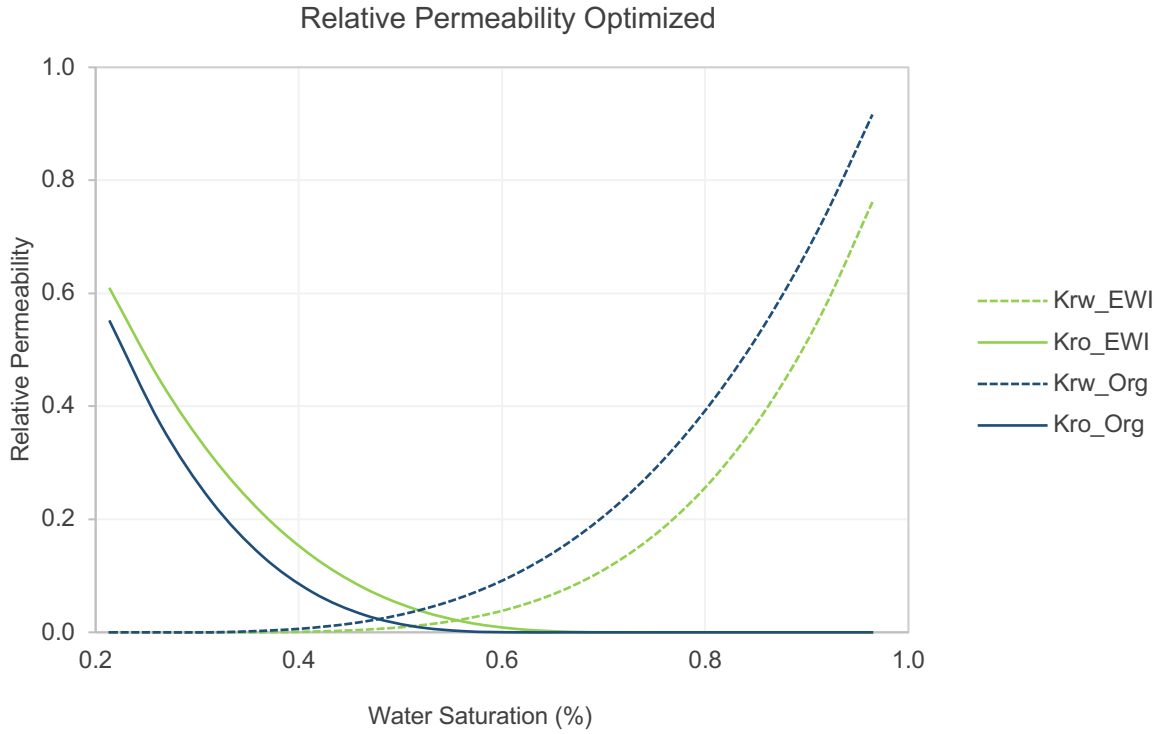
Figure 25: Optimized injection salinity.



Source: Perform by Author.

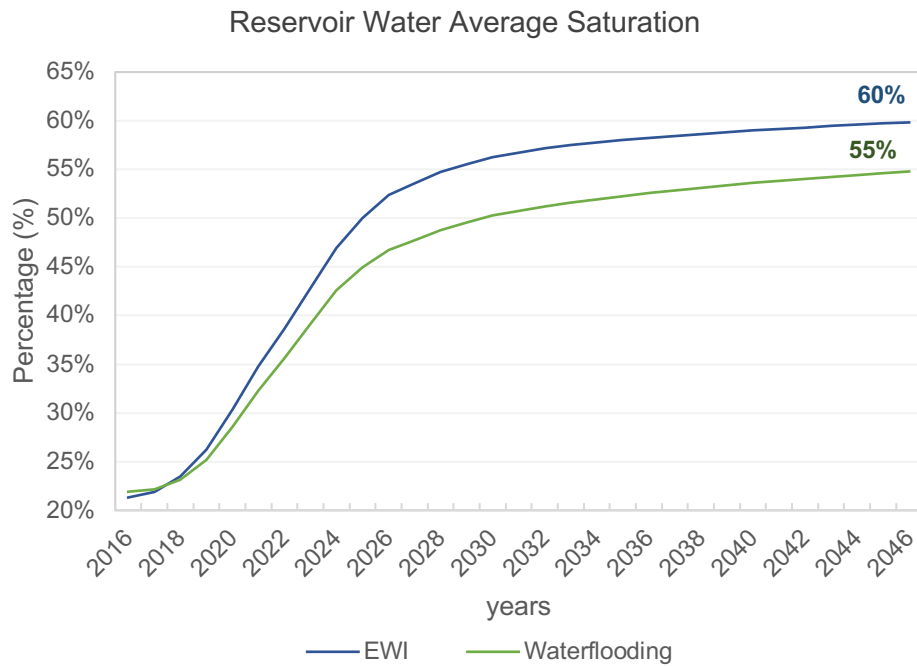
Therefore, we plot the optimized Kr curve with the salinities compared to the original (Figure 26). Here we see that the optimized result (green) had the Kro curve above the original case, increasing this permeability. Another important aspect is the reduction of the residual oil saturation, from 0.45 in the original case to 0.33 in the optimized case. The water condition is also changed, reducing Krw during all points of its saturation. Despite the significant changes, the new relative permeability still preserves characteristics of its base-case shape (Kr Original). But the analyses validate the changes for increased water wettability. The Kr resultant of optimization performed by Reginato et al. (2021) did not preserve as many features of the same original case, caused by the smaller number of features that the model of Reginato et al. (2021) used for training. These added features decrease the change in Kr shape, making sense that EWI performs simple salinity changes to promote these changes.

Figure 26: Relative Permeability after optimization vs original.



Source: Perform by Author.

Figure 27: Average water saturation during production.

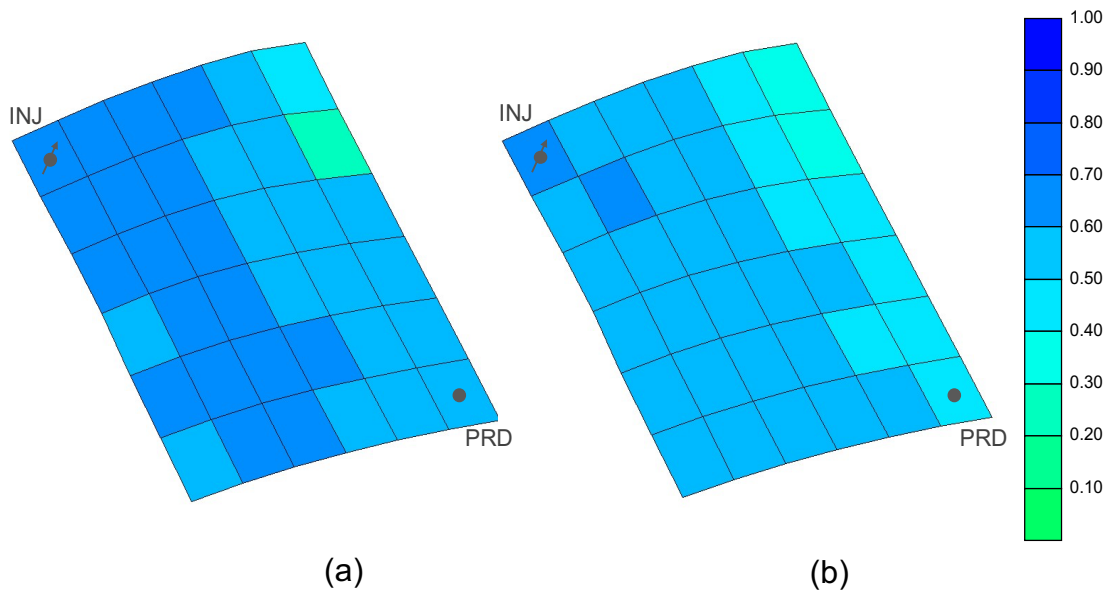


Source: Perform by Author.

The effects on production with the advanced method was also compared through the average water saturation per year of production (Figure 27). In this plot, we see an improvement of the EWI that reached higher percentages of water saturation. Therefore, we can conclude that by using the EWI method the water ended up covering a larger area of the reservoir, avoiding fingering effects. This can also be observed in the plane 17 of the simulation model at the end of production (Figure 28). More specifically, through the final water saturation in each cell, we can observe that EWI had a better performance.

Figure 28: Study Case plane 17 of 30, cell water saturation at 23/09/2046.

(a) Engineered Water Injection, (b) Waterflooding.



Source: Perform by Author.

3.5 CONCLUSIONS

The hybrid Machine Learning solution enriched the analysis Kr data analysis with the clustering approach. The investigation of clusters data shows similarities with types of wettability. The step with the three neural networks converged to ideal predictive solutions (Figure 23). This hybrid approach provided the training of three more expert networks in each cluster, which facilitates the prediction of targets but without losing its generalization ability (avoiding overfitting), validating this solution by the R^2 of validation around 0.9 scores on average. The model selection tactic (Grid Search Cross Validation) also contributed by increasing the prediction performance of the networks, despite the computational effort that testing various combinations of hyperparameters consumes.

Exploring the results of the optimizations, we see that the advanced injection method has an increase in the final NPV of 45.3% compared to the common water injection case. The advantages of using EOR injection provided an increase in oil recovery, but mainly a large reduction in production and water injection. Although EWI has the highest injection cost (25% increase), its NPV result was the highest among the cases, confirming the efficiency of using the method that, besides optimizing the variables, configured an ideal salt composition for the application. This optimized composition does not end up with a final concentration low enough to be considered Low Salinity. But this also proves that an optimized salinity can converge to concentrations that are not necessarily low, reinforcing the use of less stringent salinity limits in optimizations with this type of injection.

3.6 ACKNOWLEDGMENTS

The authors would like to thank LASG (Laboratory of Petroleum Reservoir Simulation and Management), InTRA (Integrated Technology for Rock and Fluid Analysis), and Escola Politécnica of the Universidade de São Paulo. This work was conducted with the ongoing Project registered as "Projeto de Molhabilidade e Propriedades Petrofísicas de Rochas Carbonáticas e sua Relação com a Recuperação de Hidrocarbonetos" (USP/Petrobras/ANP) funded by Petrobras, under the ANP R&D

levy as "Compromisso de Investimentos com Pesquisa e Desenvolvimento". The authors would also like to thank FAPESP (the State of São Paulo Research Foundation), and CMG[®] and MATLAB[®] for software licenses.

CHAPTER 4 – CONCLUSIONS

Applications with machine learning algorithms were successful in predicting the behavior of relative permeability parameters during EW injection. That shows a new approach to data-based modeling of complex reservoir effects, which is a simplified and agile way (Figure 12) couple effects and improve simulation accuracy. Despite the synthetic data used to train the neural networks, when we compared the ML application with the conventional geochemical methodology, was achieved high accuracy with the new approach (as we see in Figure 10). Also, we increased the training variables of the neural networks with the addition of sodium, chlorine, the formation water salinity, and mineralogical content (applied in Chapter 3), which adds more complexity to the problem, but also combine more relevant characteristics for predicting the behavior of the new Kr. Thus, the HML approach was a solution to deal with this increase in training variables. Then, the pipeline set an unsupervised classifier (the K-Means algorithm), which allowed the analysis of the characteristics of the 3 clusters by their centroids (Figure 20). In this analysis, we used Craig's rules to define the rock wettability based on Kr parameters. Thus, we observe that each centroid represents a wettability condition, so independently, the algorithm clustered the Kr following this characteristic. With the labels from clustering, we trained three neural networks for each cluster. Thus, this pipeline with two ML algorithms preserves the generalization ability without losing the forecast quality (as shown in Figure 23). The ANNs configuration using the Grid Search CV improved the prediction quality (Figure 21). Although, this method increases computational effort due to several systematic tests that the tool performs to achieve the best hyperparameters configuration.

The results of all optimizations converged for the highest NPV at EW injection. But, comparing the approach with the NNF (Chapter 2) to the HML (Chapter 3) for the case of EWI-25, we see changes in the optimized salinities. The first application used only the potential ions for modeling, and its result set the sulfate and calcium concentration higher than 5,000 ppm (Figure 13). In the second application with HML using the five salts, the salinity of the sulfate and calcium was lower, only the magnesium remained at the same levels as in the previous application, and in this case, the sodium concentration was higher than 50% of the total solution. In all applications, one or more salts had a final

concentration higher than low salinity levels, validating the argument for increasing the salinity range in optimizations.

The results with NNF compared to the original Kr present more expressive changes to a more hydrophilic condition. In the second approach (Chapter 3), we also have the changes for this hydrophilic condition (Figure 26), as the increase Kr-Oil, the decrease Kr-Water, and the residual oil saturation reduction (the endpoint of the Kr-Oil curve). This shows which relative permeability alteration to a water-wet condition is more advantageous for production, and the optimizations converged for these conditions.

The optimization algorithms used showed different results. The waterflooding case had differences in the optimized variables and final NPV, where the application with PSO obtained a better result. The NPV outcomes with the EWI-25 also varied the NPV, but this is explained by the second approach using more training variables, resulting in different optimized salinity and Kr settings. Thus, more detailed studies should be conducted to investigate these differences in results between the two optimization algorithms.

BIBLIOGRAPHY

ADEGBITE, J. O.; AL-SHALABI, E. W.; GHOSH, B. **Modeling the effect of engineered water injection on oil recovery from carbonate cores**. In: SPE INTERNATIONAL CONFERENCE ON OILFIELD CHEMISTRY, Montgomery, Texas, Apr. 2017. **Presented paper**. [S.l.]: SPE, 2017. p. 1–33. Paper n° SPE-184505-MS.

ADEGBITE, J. O.; AL-SHALABI, E. W. Optimization of engineered water injection performance in heterogeneous carbonates: a numerical study on a sector model. **Journal of Petroleum Exploration and Production Technology**, v. 10, n. 8, p. 3803-3826, Dec. 2020.

ADEGBITE, J. O.; AL-SHALABI, E. W.; GHOSH, B. Geochemical modeling of engineered water injection effect on oil recovery from carbonate cores. **Journal of Petroleum Science and Engineering**, v. 170, p. 696-711, June 2018.

AGATONOVIC-KUSTRIN, S.; BERESFORD, R. Basic concepts of artificial neural network (ANN) modeling and its application in pharmaceutical research. **Journal of Pharmaceutical and Biomedical Analysis**, v. 22, n. 5, p. 717–727, 2000.

AL-SHALABI, E. W.; SEPEHRNOORI, K.; DELSHAD, M. Simulation of wettability alteration by low-salinity water injection in waterflooded carbonate cores. **Petroleum Science and Technology**, v. 33, n. 5, p. 604–613, 2015.

ALZAYER, H.; SOHRABI, M. **Numerical simulation of improved heavy oil recovery by low-salinity water injection and polymer flooding**. [S.l: s.n.]: 2013. p. 1–13.

ARAGHINEJAD, S. **Data-driven modeling: using MATLAB® in water resources and environmental engineering**. [S.l: s.n.]: 2014. v. 67.

AUSTAD, T.; SHARIATPANAHI, S. F.; STRAND, S.; AKSULU, H.; PUNTERVOLD, T. Low salinity EOR effects in limestone reservoir cores containing anhydrite: a discussion of the chemical mechanism. **Energy and Fuels**, v. 29, n. 11, p. 6903–6911, 2015.

BABADAGLI, T. Phylosophy of EOR. **Journal of Petroleum Science and Engineering**.

v. 188, Jan. 2020.

BAI, B. Eor/ior overview. **Journal of Petroleum and Technology**, v.60, n.1, p. 42, 2008.

BANGERT, P. Introduction to Machine Learning in the Oil and Gas Industry. In: **Machine Learning and Data Science in the Oil and Gas Industry**. [S.l.]: Elsevier, 2021. Chapter 4. p. 69-81.

BERNARD, G. G. Effect of floodwater salinity on recovery of oil from cores containing clays. In: ANNUAL SPE OF AIME CALIFORNIA REGULAR MEETING, 38TH., Los Angeles, CA, 1967. [s.l.]: SPE, 1967. Related Information n° SPE- 1725;

BIDHENDI, M. M.; OLVERA, G. G.; MORIN, B.; OAKLEY, J. S.; ALVARADI V. Interfacial viscoelasticity of crude oil/brine: an alternative enhanced-oil-recovery mechanism in smart Waterflooding. **SPE Journal**, v. 23, n. 3, p. 803–818, June 2018.

BREITENBACH, E. A. Reservoir simulation : state of the art. **Journal of Petroleum Technology**, v. 43, n. 9, p. 1033-1036,1991.

BRODIE, J.; JERAULD, G. Impact of salt diffusion on low-salinity enhanced oil recovery. In: SPE SYMPOSIUM ON IMPROVED OIL RECOVERY, 19TH., 2014. **Proceedings**. [s.l.]: SPE, 2014. v. 2, p. 971-985.p. 12–16.

BROOKS, R H.; COREY, A. T. **Hydraulic properties of porous media**. Fort Collins, Colorado: Colorado State University, 1964. (Hydrology papers,n° 3). Disponível em: < https://mountainscholar.org/bitstream/handle/10217/61288/HydrologyPapers_n3.pdf>. Acesso em: Fevereiro 2021.

CHANDRASEKHAR, S.; MOHANTY, K. K. Effect of brine composition on oil-rock interaction by atomic force microscopy. **Journal of Petroleum Science and Engineering**, v. 164, p. 289–301, Febr. 2018.

CORREIA, M.; HOHENDORFF, J. GASPAR, A. T. F. S.; SCHIOZER, D. UNISIM-II-D: benchmark case proposal based on a carbonate reservoir. In: SPE Latin American and Caribbean Petroleum Engineering Conference, Quito, Equador 2015. **Presented paper**.

[s.L.] : SPE, 2015. p. 18–20.

CRAIG JR, F. F. **The reservoir engineering aspects of waterflooding**. New York: AIME, 1971.

DANG, C.; NGHIEM, L.; NGUYEN, N.; CHEN, Z.; NGUYEN Q. Mechanistic modeling of low salinity water flooding. **Journal of Petroleum Science and Engineering**, v. 146, p. 191–209, 2016.

DANG, C.; NGHIEM, L.; NGUYEN, N.; CHEN, Z; NGUYEN, Q. Modeling and optimization of low salinity waterflood. In: SPE RESERVOIR SIMULATION SYMPOSIUM, Houston, Texas, 2015. **Conference paper**. [s.L.]: SPE, 2015. v.1, p. 55-73.

DANG, C.; NGHIEM, L.; CHEN, Z.; NGUYEN, Q. Modeling low salinity waterflooding: ion exchange, geochemistry and wettability alteration. In: SPE ANNUAL TECHNICAL CONFERENCE AND EXHIBITION, New Orleans, Louisiana, 2013. **Presented paper**. [s.L.]: SPE, 2013. Paper 166447.

ESENE, C.; ONALO, D.; ZENDEHBOUDI, S.; JAMES, L.; ABORIG, A.; BUTT, S. Modeling investigation of low salinity water injection in sandstones and carbonates: Effect of Na⁺ and SO₄²⁻. **Fuel**, v. 232, p. 362–373, Mar. 2018.

EVANS, S. J. How digital engineering and cross-industry knowledge transfer is reducing project execution risks in oil and gas. In: ANNUAL OFFSHORE TECHNOLOGY CONFERENCE, May 2019, Houston, Texas. **Proceedings**. [s.L.]: OTC, 2019.

FATHI, S. J.; AUSTAD, T.; STRAND, S. Water-based enhanced oil recovery (EOR) by “smart water”: Optimal ionic composition for EOR in carbonates. **Energy and Fuels**, v. 25, n. 11, p. 5173–5179, 2011.

FJELDE, I.; ASEN, S. M.; OMEKEH, A. V. Low salinity water flooding experiments and interpretation by simulations. In: SPE IMPROVED OIL RECOVERY SYMPOSIUM, Apr. 2012. **Presented paper**. [s.L.]: SPE, 2012. Paper n°SPE-154142-MS.

GHAHRAMANI, Z. Unsupervised learning. In: BOUSQUET, O.; VON LUXBURG, U.;

RÄTSCH, G. (Org.). **Advanced lectures on machine learning: ML Summer Schools 2003**, Canberra, Australia, Febr. 2 - 14, 2003/ Tübingen, Germany, Aug. 4 - 16, 2003. Rev. ed. Berlin: Springer, 2004. p. 72–112.

GHOSH, B.; SUN, L.; OSISANYA, S. **Smart-water EOR made smarter: A laboratory development**. [s.L.:s.n.], Nov. 2016. p.14-16

GOVINDARAJU, R. S.; RAO, A. R. **Artificial neural networks in hydrology**. [s.L.]: Springer Science & Business Media, 2013. v. 36.

HAJIZADEH, Y. Machine learning in oil and gas; a SWOT analysis approach. **Journal of Petroleum Science and Engineering**, v. 176, p. 661–663, 2019.

HIRASAKI, G. J.; ZHANG, D. L. Surface chemistry of oil recovery from fractured, oil-wet, carbonate formations. **SPE Journal**, v. 9, n. 2, p. 151–162, June 2004.

JERAULD, G. R.; LIN, C. Y.; WEBB, K. J; SECCOMBE, J. C. **Modeling low salinity waterflooding**. 2008, [S.l: s.n.], 2008. p. 1–13.

JERAULD, G. R.; WEBB, L. K. J.; LIN, C-Y.; SECCOMBE, J. C. Modeling low-salinity waterflooding. In: SPE Annual Technical Conference and exhibition, San Antonio, Texas, 2006. **Presented paper**. s.L.: SPE, 2006. Paper n° SPE-102239-MS

KAYRI, M. Predictive abilities of Bayesian regularization and levenberg-marquardt algorithms in artificial neural networks: A comparative empirical study on social data. **Mathematical and Computational Applications**, v. 21, n. 224, May 2016. Article n° 21020020.

KORRANI, A. K. N.; JERAULD, G. R.; SEPEHRNOORI, K. Coupled geochemical-based modeling of low salinity waterflooding. In: SPE IMPROVED OIL RECOVERY SYMPOSIUM, 19th., Apr. 2014. **Proceedings**. s.L.: SPE, 2014. v. 2, p. 1215-1237.

LEE, K.; BOOTH, D.; ALAM, P. A comparison of supervised and unsupervised neural networks in predicting bankruptcy of Korean firms. **Expert Systems with Applications: an International Journal**, v. 29, n.1, p. 1-16, July 2005.

LIE, K. A. **An introduction to reservoir simulation using MATLAB/GNU octave.** Cambridge: University Press, 2012. v. 21.

LIKAS, A.; VLASSIS, N.; VERBEEK, J. J. The global k -means clustering algorithm. **Pattern Recognition**, v. 36, n. 2, p. 451–461, Febr. 2003.

LIU, S.; ZOLFAGHARI, A.; SATTARIN, S.; DAHAGHI, A. K.; NEGAHBAN, S. Application of neural networks in multiphase flow through porous media : predicting capillary pressure and relative permeability curves. **Journal of Petroleum Science and Engineering**, v. 180, p. 445–455, May 2019.

MADHULATHA, T S. An overview on clustering methods. **IOSR Journal of Engineering**, v. 2, n. 4, p. 719–725, Apr. 2012.

MALEKIAN, A.; CHITSAZ, N. Concepts, procedures, and applications of artificial neural network models in streamflow forecasting. In: **ADVANCES in streamflow forecasting from traditional to modern approaches.** [S.l.]: Elsevier, 2021. Chapter 4, p.115-147.

MASOUDI, R.; MOHAGHEGH, S. D.; YINGLING, D.; ANSARI, A.; AMAT, H.; MOHAMAD, N.; SABZABADI, A.; MANDEL, D. Subsurface analytics case study ; reservoir simulation and modeling of highly complex offshore field in Malaysia, using artificial intelligent and machine learning subsurface analytics top-down modeling. In: SPE ANNUAL TECHNICAL CONFERENCE AND EXHIBITION , Oct. 2020. **Presented paper.** s.L.: SPE, 2020. Paper n SPE 201693-MS.

MIRZAEI-PAIAMAN, A. New methods for qualitative and quantitative determination of wettability from relative permeability curves : revisiting Craig’s rules of thumb and introducing Lak wettability index. **Fuel**, v. 288, p. 1-15, 2021. Article 119623,

MOHAGHEGH, S.; AMERI, S. **Artificial neural network as a valuable tool for petroleum engineers.** [s. L]: Society of Petroleum Engineers, 1995. 6 p. SPE 29220

MOHAGHEGH, S. Virtual-intelligence applications in petroleum engineering : part 1 — Artificial neural networks. **Journal of Petroleum Technology**, v. 52, n. 9, p. 64-73, Sept. 2000. Paper n SPE 58046-JPT

MORISSETTE, L.; CHARTIER, S. The k-means clustering technique: general considerations and implementation in Mathematica. **Tutorials in Quantitative Methods for Psychology**, v. 9, n. 1, p. 15–24, 2013.

MORROW, N. R.; TANG, G.; VALAT, M.; XIE, X. Prospects of improved oil recovery related to wettability and brine composition. **Journal of Petroleum Science and Engineering**, v. 20, n. 3–4, p. 267–276, 1998.

MOSALLANEZHAD, A.; KALANTARIASL, A. Geochemical simulation of single-phase ion-engineered water interactions with carbonate rocks : implications for enhanced oil recovery. **Journal of Molecular Liquids**, v. 341, p. 1-16, 2021. Article 117395.

MUSTAFIZ, S.; ISLAM, M. R. State-of-the-art petroleum reservoir simulation. **Petroleum Science and Technology**, v. 26, n. 10–11, p. 1303–1329, 2008.

NGUYEN, H.; BUI, X.; BUI, H.; MAI, N. A comparative study of artificial neural networks in predicting blast-induced air-blast overpressure at Deo Nai open-pit coal mine, Vietnam. **Neural Computing and Applications**, v. 32, n. 8, p. 3939–3955, 2020.

OMEKEH, A.; FRIIS, H. A.; FJELDE, I.; EVJE, S. Modeling of ion-exchange and solubility in low salinity water flooding. In: SPE IMPROVED OIL RECOVERY SYMPOSIUM, 18TH., 2012. **Proceedings**. [s. L.]: SPE, 2012. p. 1–13. v. 2, p. 990-1002.

REGINATO, L. F.; CARNEIRO, C. C.; GIORIA, R. S.; SAMPAIO, M. Prediction of wettability alteration using the artificial neural networks in the salinity control of water injection in carbonate reservoirs. In: OFFSHORE TECHNOLOGY CONFERENCE BRASIL, Rio de Janeiro, Oct. 2019. **OTCB 2019**. [s.L.: s.n.], 2019.

REGINATO, L. F.; PEDRONI, L. G.; COMPAN, A. L. M.; SKINNER, R.; SAMPAIO, M. A. Optimization of ionic concentrations in engineered water injection in carbonate reservoir through ANN and FGA. **Oil and Gas Science and Technology - Rev. IFP Energies Nouvelles**, v. 76, p. 1-14, 2021. Article13.

ROSTAMI, P.; MEHRABAN, M. F.; SHARIFI, M.; DEJAM, M; AYATOLLAHI, S.. Effect of

water salinity on oil / brine interfacial behaviour during low salinity waterflooding : A mechanistic study. **Petroleum**, v. 5, n. 4, p. 367-374, Dec. 2019.

SAIKIA, B. D.; MAHADEVAN, J.; RAO, D. N. Exploring mechanisms for wettability alteration in low-salinity waterfloods in carbonate rocks. **Journal of Petroleum Science and Engineering**, v. 164, p. 595–602, 2018.

SAMPAIO, M. A.; BARRETO, C. E.A.G.; SCHIOZER, D. J. Assisted optimization method for comparison between conventional and intelligent producers considering uncertainties. **Journal of Petroleum Science and Engineering**, v. 133, p. 268–279, 2015.

SEETHEPALLI, A.; ADIBHATLA, B.; MOHANTY, K. K. Physicochemical interactions during surfactant flooding of fractured carbonate reservoirs. **SPE Journal**, v. 9, n. 4, p. 411–418, 2004.

SHOBHA, G. ; RANGASWAMY, S. Machine learning. In: RAO,C. R. (Ed.). **Computational analysis and understanding of natural languages: principles, methods and applications**. [s. L.]: North Holland, 2018. Cap. 9. (Handbook of Statistics, v.38).

STRAND, S.; HØGNESEN, E. J.; AUSTAD, T. Wettability alteration of carbonates - Effects of potential determining ions (Ca^{2+} and SO_4^{2-}) and temperature. **Colloids and Surfaces A: Physicochemical and Engineering Aspects**, v. 275, n. 1–3, p. 1–10, Mar. 2006.

STRIK, D. P. B. T. B.;DOMNANOVICH, A. M.; ZANI, L.; BRAUN, R.; HOLUBAR, P. Prediction of trace compounds in biogas from anaerobic digestion using the MATLAB Neural Network Toolbox. **Environmental Modelling and Software**, v. 20, n. 6, p. 803–810, June 2005.

SULEIMANOV, B. A.; LATIFOV, Y. A.; VELIYEV, E. F.; FRAMPTON, H. Comparative analysis of the EOR mechanisms by using low salinity and low hardness alkaline water. **Journal of Petroleum Science and Engineering**, v. 162, p. 35–43, Aug. 2018.

TALABIS, M. R. M.; MCPHERSON, R.; MIYAMOTO, I.; MARTIN, J. L.; KAYE, D.

Information security analytics. [s.L.]: Syngress, 2015. p. 1–12: Analytics defined.

WEBB, K. J.; BLACK, C. J. J.; EDMONDS, I. J. Low salinity oil recovery – the role of reservoir condition corefloods. In: EUROPEAN SYMPOSIUM ON IMPROVED OIL RECOVERY, 13TH., Budapest, Hungary, Apr. 2005. **Conference proceedings:** IOR 2005. s.L.: European Association of Geoscientists & Engineers, 2005. p. 95-101.

WEBB, K. J.; BLACK, C. J. J.; A-AJEEL, H. Low salinity oil recovery-log-inject-log. In: SPE SYMPOSIUM ON IMPROVED OIL RECOVERY, Tulsa, Apr. 2004. **Proceedings.** [s. L.]: SPE, 2004. Paper SPE 89379-MS.

WEBB, K. J.; BLACK, C. J. J.; EDMONDS, I. J. Low salinity oil recovery – the role of reservoir condition corefloods. In: EUROPEAN SYMPOSIUM ON IMPROVED OIL RECOVERY, 13TH., Budapest, Hungary, Apr. 2005. **Conference proceedings:** IOR 2005. [s.L.]: European Association of Geoscientists & Engineers, 2005. CP-12-00045.

WEBB, K.; LAGER, A.; BLACK, C. Comparison of high / low salinity water / oil relative permeability. In: INTERNATIONAL SYMPOSIUM OF THE SOCIETY OF CORE ANALYSTS, Abu Dhabi, UAE, Oct.- Nov. 2008. **Presented paper.** [s.L.]: BP Exploration, 2008. p. 1-8. Paper SCA2008-39 1/12.

XIAO, R.; GUPTA, R.; GLOTZBACH, R. C.; SINHA, S.; TELETZKE, G. F. Evaluation of low-salinity waterflooding in Middle East carbonate reservoirs using a novel, field-representative coreflood method. **Journal of Petroleum Science and Engineering**, v. 163, p. 683–690, Apr. 2018.

YASEEN, Z. M.; EI-SHAFIE, A.; JAAFAR, O.; AFAN, H. A.; SAYL, K. N. Artificial intelligence based models for stream-flow forecasting: 2000-2015. **Journal of Hydrology**, v. 530, p. 829–844, 2015.

YOUSEF, A. A.; AL-SALEH, S.; AL-JAWFI, M. S. Smart waterflooding for carbonate reservoirs: salinity and role of ions. In: SPE MIDDLE EAST OIL AND GAS SHOW AND CONFERENCE, 17TH., Manama, Bahrain, 2011. **Presented paper.** [s.L.]: SPE, 2011. p. 632-642. Paper SPE n° 141082-MS.

YOUSEF, A. A.; AL-SALEH, S.; AL-KAABI, A.; AL-JAWFI, M. Laboratory investigation of novel oil recovery method for carbonate reservoirs. In: CANADIAN UNCONVENTIONAL RESOURCES AND INTERNATIONAL PETROLEUM CONFERENCE, Calgary, 2010. **Conference proceedings**. [s.L.]: Society of Petroleum Engineers, 2010. v. 3, p.1825-1859.

YOUSEF, A. A.; LIU, J.; BLANCHARD, G.; AL-SALEH, S.; AL-ZAHRANI, T.; AL-ZAHRANI, R.; AL-TAMMAR, H.; AL-MULHIM, N. SmartWater flooding : industry's first field test in carbonate reservoirs. In: SPE ANNUAL TECHNICAL CONFERENCE AND EXHIBITION, San Antonio, Texas, 2012. **Presented paper**. [s.L.]: SPE, Oct. 2012. p. 8–10. Paper n° 159526-MS.

ZHANG, P.; TWEHEYO, M. T.; AUSTAD, T. Wettability alteration and improved oil recovery by spontaneous imbibition of seawater into chalk : impact of the potential determining ions Ca^{2+} , Mg^{2+} , and SO_4^{2-} . **Colloids and Surfaces A: Physicochemical and Engineering Aspects**, v. 301, p. 199–208, 2007.

ZHANG, P.; TWEHEYO, M. T.; AUSTAD, T. Wettability alteration and improved oil recovery in chalk : the effect of calcium in the presence of sulfate. **Energy and Fuels**, v.20, n. 5, p. 2056-2062, Sept. 2006.